

# Formation of transformation products during ozonation of secondary wastewater effluent and their fate in post-treatment: From laboratory- to full-scale

Rebekka Gulde<sup>a</sup>, Moreno Rutsch<sup>a</sup>, Baptiste Clerc<sup>a</sup>, Jennifer E. Schollée<sup>a</sup>, Urs von Gunten<sup>a,b,c</sup>, Christa S. McArdell<sup>a,\*</sup>

<sup>a</sup> Eawag, Swiss Federal Institute of Aquatic Science and Technology, CH-8600 Dübendorf, Switzerland

<sup>b</sup> School of Architecture, Civil and Environmental Engineering (ENAC), Ecole Polytechnique Fédérale de Lausanne (EPFL), CH-1015 Lausanne, Switzerland

<sup>c</sup> Institute of Biogeochemistry and Pollutant Dynamics (IBP), ETH Zurich, CH-8092 Zurich, Switzerland

## ARTICLE INFO

### Article history:

Received 24 February 2021

Revised 21 April 2021

Accepted 27 April 2021

Available online 5 May 2021

### Keywords:

Ozone

Granular activated carbon

Powdered activated carbon

Sand filter

Micropollutants

Structure elucidation

## ABSTRACT

Ozonation is increasingly applied in water and wastewater treatment for the abatement of micropollutants (MPs). However, the transformation products formed during ozonation (OTPs) and their fate in biological or sorptive post-treatments is largely unknown. In this project, a high-throughput approach, combining laboratory ozonation experiments and detection by liquid chromatography high-resolution mass spectrometry (LC-HR-MS/MS), was developed and applied to identify OTPs formed during ozonation of wastewater effluent for a large number of relevant MPs (total 87). For the laboratory ozonation experiments, a simplified experimental solution, consisting of surrogate organic matter (methanol and acetate), was created, which produced ozonation conditions similar to realistic conditions in terms of ozone and hydroxyl radical exposures. The 87 selected parent MPs were divided into 19 mixtures, which enabled the identification of OTPs with an optimized number of experiments. The following two approaches were considered to identify OTPs. (1) A screening of LC-HR-MS signal formation in these experiments was performed and revealed a list of 1749 potential OTP candidate signals associated to 70 parent MPs. This list can be used in future suspect screening studies. (2) A screening was performed for signals that were formed in both batch experiments and in samples of wastewater treatment plants (WWTPs). This second approach was ultimately more time-efficient and was applied to four different WWTPs with ozonation (specific ozone doses in the range 0.23–0.55 gO<sub>3</sub>/gDOC), leading to the identification of 84 relevant OTPs of 40 parent MPs in wastewater effluent. Chemical structures could be proposed for 83 OTPs through the interpretation of MS/MS spectra and expert knowledge in ozone chemistry. Forty-eight OTPs (58%) have not been reported previously. The fate of the verified OTPs was studied in different post-treatment steps. During sand filtration, 87–89% of the OTPs were stable. In granular activated carbon (GAC) filters, OTPs were abated with decreasing efficiency with increasing run times of the filters. For example, in a GAC filter with 16,000 bed volumes, 53% of the OTPs were abated, while in a GAC filter with 35,000 bed volumes, 40% of the OTPs were abated. The highest abatement (87% of OTPs) was observed when 13 mg/L powdered activated carbon (PAC) was dosed onto a sand filter.

© 2021 The Authors. Published by Elsevier Ltd.

This is an open access article under the CC BY license (<http://creativecommons.org/licenses/by/4.0/>)

## 1. Introduction

Oxidative treatment such as ozonation has been applied in water treatment for decades. Traditionally, ozone-based technologies were mainly applied for disinfection of drinking waters, but since the 1990s, the possibility to simultaneously abate micropollutants

(MPs) (mainly with ozone or ozone-based advanced oxidation processes (AOPs) involving OH radicals (•OH)) has gained importance (von Sonntag and von Gunten 2012). The same processes are currently being evaluated and increasingly applied for enhanced treatment of municipal wastewater effluents (von Gunten 2018). While initially the abatement of parent compounds was the sole goal of such treatments, the fact that MPs are not mineralized during reactions with ozone and/or •OH, but largely unknown transformation products are formed, required a paradigm shift (von Gunten

\* Corresponding author.

E-mail address: [christa.mcardell@eawag.ch](mailto:christa.mcardell@eawag.ch) (C.S. McArdell).

2003, 2018). In previous studies, *in vitro* bioassays revealed significantly reduced ecotoxicological effects after ozonation of secondary wastewater effluents (Margot et al. 2013), and it has been shown that the formed transformation products have lower biological activity (e.g., antimicrobial, estrogenic or herbicidal activity) compared to the parent compounds (Lee and von Gunten 2016). However, some studies showed an increased toxicity after ozonation (Magdeburg et al. 2014, Stalter et al. 2010), and it is unknown to what extent transformation products from MPs or by-products formed during oxidation of matrix components (i.e., dissolved organic matter, DOM) are involved in these observations (Lee and von Gunten 2016, Mestankova et al. 2011, Mestankova et al. 2014, Mestankova et al. 2012, von Gunten 2018). Fortunately, increased ozonation-induced toxicity is often abated during biological post-treatment (Stalter et al. 2010). Since assimilable organic carbon (AOC) or biodegradable dissolved organic carbon (BDOC), which is formed during ozonation, is usually well-degraded in the biological post-treatment, it can be assumed that a significant portion of the induced toxicity is related to compounds contributing to these bulk parameters (Zimmermann et al. 2011). In analogy to AOC or BDOC, it is often assumed that ozonation transformation products (OTPs) are well-biodegradable; however, this and their potential contribution to the increased toxicity are still largely unknown. Therefore, it is recommended to test the feasibility of ozonation at a specific WWTP, before its installation, with a test procedure including chemical and ecotoxicological parameters (Schindler Wildhaber et al. 2015).

Based on general knowledge of ozone chemistry, OTPs resulting from the reaction of ozone with certain structural moieties can be predicted based on their reactivity in systems where only ozone is considered (Lee et al. 2017). However, under realistic conditions, ozone decomposes to  $\bullet\text{OH}$  (von Sonntag and von Gunten 2012), which concurrently react less selectively with the MPs or with the OTPs formed from the direct reaction with ozone, complicating the prediction of OTPs.

Typically, liquid chromatography coupled to high-resolution tandem mass spectrometry (LC-HR-MS/MS) is applied for the identification of OTPs. OTPs can be elucidated in laboratory experiments often in combination with expert knowledge and/or model predictions (Lee et al. 2017, von Gunten 2018). However, the elucidation of OTPs of single substances is very labor-intensive and therefore data remain scarce (Carbajo et al. 2015, Christophoridis et al. 2016, Knopp et al. 2016, Rodayan et al. 2014, Rosal et al. 2009). Moreover, OTPs that are elucidated in laboratory experiments at specific ozone exposures in the absence of  $\bullet\text{OH}$  reactions might not occur or occur in different yields in real water matrices because of the contribution of  $\bullet\text{OH}$  to product formation (Acero et al. 2000, Kamath et al. 2018, Stefan and Bolton 1998, Stefan et al. 2000). For example, during ozonation of secondary effluent at WWTP Neugut with 2 mg/L ozone, a yield of about 40% of chlorothiazide from the transformation of hydrochlorothiazide was observed, while in laboratory experiments where  $\bullet\text{OH}$  were scavenged the yield of chlorothiazide was >80% (Borowska et al. 2016). Different OTPs may be favored in realistic samples with varying types and concentrations of DOM determining the ozone and  $\bullet\text{OH}$  exposures, compared to laboratory experiments performed in absence of  $\bullet\text{OH}$ . Ozone and  $\bullet\text{OH}$  exposure at a dissolved organic carbon (DOC)-normalized ozone dose, together with the rate constants for the reactions of selected MPs with ozone and  $\bullet\text{OH}$ , were found to be key parameters to predict the abatement efficiency of the MPs during ozonation of municipal wastewater effluents (Lee et al. 2013).

Non-target analysis with LC-HR-MS/MS can be used to screen for peaks that appear after ozonation in laboratory-, pilot- or full-scale studies (Brunner et al. 2020, Gago-Ferrero et al. 2015, Itzel et al. 2020, Krauss et al. 2010, Phungsai et al. 2016,

Schollée et al. 2018, Schollée et al. 2021b). However, with this approach, it is very difficult to assign chemical structures to transformation product candidates and to relate transformation products to their parent MPs. It is also challenging to differentiate between the OTPs arising from the reaction of ozone with MPs and those that are formed as oxidation by-products from the water matrix components.

Furthermore, it is not easily predictable how stable the formed products are when the oxidants are depleted and what their fate is in (biological) post-treatment processes, which typically follow an ozonation process (Hübner et al. 2015). Overall, there is an important knowledge gap related to the formation of OTPs during ozonation and their fate during post-treatment in wastewater treatment plant (WWTP) effluents.

The goal of this study was to identify OTPs that are formed during ozonation of secondary WWTP effluent from a large number of MPs and to assess their fate in different post-treatments. A novel method was developed that enables an efficient and reliable identification of relevant OTPs formed during ozonation of MPs, including the elucidation of their chemical structures. To identify OTPs, laboratory ozonation batch experiments were performed in simulated water matrices (with similar ozone- and  $\bullet\text{OH}$  exposures as in wastewater samples) with “smart” mixtures of MPs that enabled backtracking of parent MPs, without needing an individual experiment for each MP. In parallel, wastewater samples were collected from four WWTPs equipped with ozonation in full- or pilot-scale and different post-treatment technologies, namely sand filtration, granular activated carbon (GAC) filtration, and treatment with powdered activated carbon (PAC) dosed onto a sand filter. All samples were measured with LC-HR-MS/MS. Two approaches were tested to identify OTP signals that were formed in laboratory ozonation batch experiments and during ozonation in the WWTPs. The structures of identified OTP signals were elucidated by interpretation of the MS<sup>2</sup> spectra, as well as expert knowledge on ozone chemistry. The abatement of the OTPs in the differing post-treatment steps was evaluated using the relative difference of the corresponding peak areas.

## 2. Material and methods

### 2.1. Selection of micropollutants and their distribution into “smart” mixtures

Eighty-seven organic MPs were selected based on their abundance in municipal wastewater effluents (Bourgin et al. 2018) and their relevance in aquatic ecosystems (Hollender et al. 2018). An additional criterion for the selection of MPs was the presence of different functional moieties in their chemical structures that are known to react with ozone, such as primary, secondary and tertiary amines, olefins, activated aromatic compounds, and thioethers (von Sonntag and von Gunten 2012). The selected MPs are mainly pharmaceuticals and pesticides. The 87 MPs were separated into 19 different mixtures, whereby each MP was present in two mixtures, while no other MP occurred twice in these two mixtures (details in Text S1, Figs. S1 and S2, SI). The following MPs were selected: 2,4-dichlorophenoxyacetic acid (24D), 2,7-naphthalic disulfonic acid (27N), 2-naphthalic sulfonic acid (2NS), 4/5-methylbenzotriazole (TBZ), acesulfame (ACE), aliskiren (ALI), amisulpride (ASP), amitriptyline (ATT), atazanavir (ATA), atenolol (ATE), atenolol acid (ACD), atenolol-desisopropyl (ADI), atrazine (ATZ), benisothiazolone (BIT), benzophenone-3 (BZP), benzotriazole (BZT), bezafibrate (BZF), candesartan (CAN), carbamazepine (CBZ), cephalixin (CPX), cetirizine (CET), citalopram (CIT), clarithromycin (CLA), clindamycin (CLI), clozapine (CLO), codeine (COD), caffeine (COF), cyprodinil (CYP), diclofenac (DIC), diltiazem (DIL), diphenhydramine (DIP), diuron (DIU), efavirenz (EFA),

emtricitabine (EMT), eprosartan (EPR), etodolac (ETO), fenfluramine (FFA), fenpropidin (FEN), flecainide (FLE), flufenamic acid (FAD), gabapentin (GAB), hydrochlorothiazide (HCT), ibuprofen (IBU), irbesartan (IRB), ketoprofen (KET), lamotrigine (LAM), levamisole (LVI), levetiracetam (LTA), lidocaine (LID), mecoprop (MEC), mefenamic acid (MAA), metformin (MET), methoxyfenozide (MFO), methylprednisolone (MPN), metoprolol (MTO), mycophenolic acid (MYA), napropamide (NPP), naproxen (NAP), *N*-bisdesmethyl tramadol (BDT), *N*-desmethyltramadol (DMT), norfenfluramine (NFF), norlidocaine (NLI), oseltamivir (OSE), oxazepam (OXA), oxcarbazepine (OXC), phenazone (PHE), pravastatin (PRA), progesterone (PGR), prometon (PRM), propranolol (PRO), propylamide (PYZ), ranitidine (RAN), resveratrol (RES), rosuvastatin (ROS), sitagliptin (SIT), sucralose (SUC), sulfamethazine (SMZ), sulfamethoxazole (SMX), sulfapyridine (SPD), sulpiride (SUL), thiaclopride (THI), tramadol (TRA), triclosan (TCL), trimethoprim (TRI), valsartan (VAL), valsartan acid (VAA), and venlafaxine (VEN).

## 2.2. Laboratory ozonation batch experiments

### 2.2.1. Simulation of water matrix containing organic matter

A simplified organic water matrix was simulated by substituting the organic matter with methanol (radical chain carrier) and acetate (radical chain inhibitor) (Staelin and Hoigne 1985). This matrix yields experimental solutions with ozonation conditions similar to real water matrices in terms of ozone and  $\bullet\text{OH}$  exposures (and concentration ratios  $\bullet\text{OH}/\text{O}_3$  known as  $R_{\text{ct}}$  (Elovitz and von Gunten 1999)), but with less interferences in the LC-HR-MS/MS screening for OTP signals. The experimental solution consisted of 0.15 mM acetate and 0.029 mM methanol in phosphate buffer (1–5 mM depending on the experiment) adjusted to pH 7.5. Ozone exposure at full depletion was 0.035 Ms with an  $R_{\text{ct}}$  of  $1.3 \times 10^{-8}$ , representative for an environmental matrix (Elovitz et al. 2000, Lee et al. 2013). Details of this approach and another simulated matrix are provided in Text S2, Table S4, and Figs. S3–S9, SI.

### 2.2.2. Ozonation batch experiments

Two types of ozonation batch experiments were conducted. The first set of 19 ozonation batch experiments was spiked with the 19 different MP mixtures as described in Section 2.1. These experiments are called *O3bMix* in the following and they were used to relate OTPs to the respective parent MPs. We targeted a final concentration of 10  $\mu\text{g/L}$  for each MP (0.013–0.084  $\mu\text{M}$ ). Additionally, a second set of ozonation batch experiments was conducted where all MPs were spiked together to a final target concentration of 1  $\mu\text{g/L}$  each. These experiments are called *O3bAll* in the following. The *O3bAll* samples were analyzed concurrently with the WWTP samples and processed simultaneously to enable an efficient screening for OTP candidate signals. The following experimental set-up was similar for both types of ozonation batch experiments (*O3bMix* and *O3bAll*). The MP spike solution (*O3bMix*: 32  $\mu\text{L}$  of 100 mg/L stock solution in methanol, *O3bAll*: 40  $\mu\text{L}$  of 8 mg/L stock solution in methanol) was added to an empty 250 mL Schott bottle and left under a gentle nitrogen stream in the dark for 1–3 days to evaporate the organic solvent. Afterwards, 250 mL of the experimental solution (described in Section 2.2.1), augmented with 0.5  $\mu\text{M}$  para-chlorobenzoic acid (pCBA), was added. For the dissolution of the MPs, the solution was kept on a circular shaker table at 130 rpm overnight.

The ozonation batch experiments were adopted from Lee et al. (2013). Briefly, we initiated the experiment by adding an ozone stock solution to a concentration of 1.3 mg  $\text{O}_3/\text{L}$  in 250 mL batch reactors. To follow the evolution of the reactions, aliquots (6 mL) were taken at multiple time points. To quench ozone in these samples, quenching reagents were previously added into the sample vials. Two kinds of quenching reagents were used.

First, samples quenched with indigo were taken (sampling times: before ozone addition, 15, 45, 90, 150, 240, 300, 480, 900, 1800 seconds after ozone addition) to determine the residual ozone concentration via the indigo method (Bader and Hoigné 1981). From these, the ozone exposures were obtained from the area under the ozone decay curves (von Gunten and Hoigné 1994). Second, samples quenched with sulfite (final concentration 0.16 mM) were taken (sampling times: before ozone addition, 23, 53, 98, 158, 248, 308, 488, 908, 1808 seconds after ozone addition) to determine the  $\bullet\text{OH}$  exposures and consequently the  $R_{\text{ct}}$  value from the abatement of the ozone-recalcitrant compound pCBA measured with high-performance liquid chromatography coupled to an UV-VIS detector (Ultimate 3000, Thermo Scientific) (Elovitz and von Gunten 1999, Elovitz et al. 2000). In addition, five of these sulfite-quenched samples (sampling times: before ozone addition, 53, 158, 308, 488 seconds after ozone addition) were used for analyses by LC-HR-MS/MS as described in Section 2.4. Unfortunately, the ozone quenching with sulfite did not work in the *O3bMix* samples (the sulfite solution was not fresh enough, i.e., prepared a few hours before the start of the experiment). Therefore, all samples, except those collected prior to ozone addition, reacted to full ozone depletion (around 15–30 min). Therefore, only one time-point was available and a time-dependent evaluation of OTP formation was not possible in the *O3bMix* samples. The *O3bAll* experiments were not affected.

## 2.3. Wastewater treatment plant samples

Four municipal WWTPs in Switzerland with advanced treatment were sampled after biological treatment (BIO), after ozonation (OZO) and after a post-treatment (EFF). One WWTP (Neugut, Dübendorf) operates a full-scale ozonation followed by sand filtration (SF), while the other three WWTPs operated pilot plants with a low-dose pre-ozonation, followed by activated carbon treatment, either with GAC filtration (GAC1 at WWTP Glarnerland, Bilen, and GAC2 at WWTP Altenrhein, Altenrhein) or with powdered activated carbon (PAC) dosed on a sand filter (PAC at WWTP ProReno, Basel). At WWTP Neugut (described in detail in Bourgin et al. (2018)), two flow-proportional 24 h composite samples (pH 6.8–7.9), taken on March 10, 2015 (transferred ozone 2.76 mg/L or 0.55 g $\text{O}_3/\text{gDOC}$  at 5.0 mg/L DOC) and on April 14, 2015 (transferred ozone 2.74 mg/L or 0.50 g $\text{O}_3/\text{gDOC}$  at 5.5 mg/L DOC), were used for analysis. WWTP Glarnerland operated a pilot plant with pre-ozonation at low dose followed by a GAC filter (empty bed contact time of approximately 24 minutes, called GAC1) containing the GAC-Type Pool W1–3 (CarboTech AC GmbH) sieved to a particle size of 0.85–2 mm (10  $\times$  20 mesh) (McArdell et al. 2020, Ultramaré et al. 2021). Three flow-proportional 24 h composite samples taken on November 21, 2017 (transferred ozone 2.57 mg/L or 0.33 g $\text{O}_3/\text{gDOC}$  at 5.4 mg/L DOC, GAC at 16,278 bed volumes (BV), pH 7.9), April 18, 2018 (transferred ozone 4.08 mg/L or 0.33 g $\text{O}_3/\text{gDOC}$  at 10.7 mg/L DOC, GAC at 24,679 BV, pH 8.2) and October 17, 2018 (transferred ozone 2.79 mg/L or 0.23 g $\text{O}_3/\text{gDOC}$  at 8.7 mg/L DOC, GAC at 35,282 BV, pH 7–8) were used for analysis. Since significant nitrite concentrations were measured in the effluent of this WWTP, the applied ozone dose was corrected by ozone consumption for nitrite oxidation. WWTP Altenrhein operated a pilot plant with pre-ozonation at low dose followed by a GAC filter (empty bed contact time 20 minutes, called GAC2) containing Cyclecarb 401 (Virgin, Chemviron Carbon) with a particle size of 0.425–2.36 mm (8  $\times$  40 mesh) (Schollée et al. 2021b). One flow-proportional 24 h composite sample taken on September 5, 2018 (applied ozone 2.22 mg/L or 0.29 g $\text{O}_3/\text{gDOC}$  at 7.6 mg/L DOC, transferred >90%, GAC at 48,154 BV, pH 7.9). WWTP ProReno, treating 90% municipal wastewater mixed with 10% industrial wastewater, operated a pilot plant using a sequencing batch reactor (SBR) with



low-dose pre-ozonation followed by PAC addition onto a sand filter (called PAC) (Krahnstöver et al. 2018, Schollée et al. 2021b). One flow-proportional 24 h composite sample was taken on April 20, 2017 (applied ozone 1.5 mg/L or 0.21 gO<sub>3</sub>/gDOC at 7 mg/L DOC and a PAC dose of 13 mg/L onto a sand filter, pH 7.5–8.0). All samples were kept frozen at -20°C until analyses.

## 2.4. Chemical analyses

In general, reverse-phase liquid chromatography coupled to a high-resolution quadrupole Orbitrap mass spectrometry (LC-HR-MS/MS) was used for chemical analyses. The acquisition method of the *O3bMix* samples that were used to relate OTPs to their respective parent MPs differed slightly from the acquisition method of the *O3bAll* and the WWTP samples, which were used in combination to (i) identify OTPs forming in *O3bAll* and the WWTP samples and (ii) to elucidate the structures via the acquired MS<sup>2</sup> scans.

### 2.4.1. Method for the *O3bMix* samples

After ozonation, 1 mL from each *O3bMix* sample was taken and augmented with 20 µL internal standard (ISTD) stock solution (250 µg/L in methanol and ethanol, for details on the ISTDs, see Table S1, SI) and stored at 4°C in the dark. The analytical method was adopted from Gulde et al. (2014). A sample aliquot of 100 µL was directly injected onto a C18 Atlantis T3 column (particle size 3 µm, 3.0 × 150 mm, Waters) without enrichment (MP concentration was 10 µg/L before ozonation). A gradient of nanopure water and methanol, both augmented with 0.1% formic acid, enabled chromatographic separation. The eluate of the first 4 minutes was discarded to avoid salts from the phosphate buffer from entering the HR-MS instrument (Qexactive+, Thermo Scientific). Detection was performed by full scan acquisition with a mass resolution (R) of 140 000 (at *m/z* 200) and data-dependent MS/MS (R = 17 500, Top 10). The scan range was 50–750 *m/z* and the dynamic exclusion was set to 3 s. Data-dependent MS<sup>2</sup> were triggered at masses of OTPs predicted by O3-PPS (Lee et al. 2014, Schollée et al. 2021a). Samples were measured in separate runs for positive and negative electrospray ionization, whereby nine calibration standards (0.1, 0.25, 0.5, 1, 2.5, 5, 10, 25, 50 µg/L) were acquired in switch mode with R = 70 000 (details on method and MP quantification in Text S3.1 and Table S1, SI).

### 2.4.2. Method for the *O3bAll*, the re-measurement of the *O3bMix*, and the WWTP samples

The *O3bAll*, the re-measured *O3bMix*, and the WWTP samples were enriched by online solid phase extraction (SPE) prior to the LC-HR-MS/MS measurement as described by Bourgin et al. (2018), using 20 mL samples. *O3bAll* samples (MP concentration of 1 µg/L before ozonation) were obtained by taking 2–5 mL of the sulfite quenched sample, adding 16 µL ISTD stock solution (250 µg/L) and filling them up with nanopure water to a volume of 20 mL. *O3bMix* samples were re-measured with this method for MS<sup>2</sup> acquisition and for relating OTPs to their respective parent MPs. Here, 16 µL ISTD stock solution (250 µg/L) and 17.5 mL nanopure water were added to a 2.5 mL sample. This procedure resulted in *O3bMix* samples with concentrations 25 times higher than in the direct measurements. The WWTP samples were filtered through two glass microfiber filters, i.e., GF/D (top, 2.7 µm pore size, Whatman) and GF/F (bottom, 0.7 µm pore size, Whatman). The filtrate (50 mL) was diluted with 50 mL nanopure water and spiked with 80 µL ISTD stock solution (250 µg/L). The SPE cartridge was filled with four absorbents (9 mg Oasis HLB and 9 mg of a mixture of Strata-X-AW/Strata-X-CW/ENV 1/1/1.5). The cartridge was eluted with methanol containing 0.1% formic acid. The extracts were chromatographically separated on a C18 Atlantis T3 column (particle size 5 µm, 3.0 × 150 mm, Waters) using a gradient of nanopure

water and methanol both acidified with 0.1% formic acid as eluents. HR-MS and MS/MS acquisition were obtained by a Qexactive instrument (Thermo Scientific) with R = 140 000 (*m/z* 200) and data-dependent MS/MS (R = 17 500, Top 7). The scan range was 60–900 *m/z* and the dynamic exclusion window was set to 5 s. Data-dependent MS<sup>2</sup> were triggered at identified OTP masses (see Section 2.5 for details). Samples were measured in separate runs for positive and negative electrospray ionization. A calibration row consisting of eleven standards (1, 2.5, 5, 10, 25, 50, 100, 250, 500, 750, 1000 ng/L) was measured at the beginning of each run (for details on method and MP quantification, see Text S3.2 and Table S1, SI).

## 2.5. Identification of ozonation transformation products

In principle, OTPs can be identified in WWTP samples by the two approaches shown in Fig. 1. Approach 1 resulted in a list of suspect OTPs by selecting signals that were formed in the *O3bMix* experiments for each parent MP (Approach 1A–C). Due to time constraints, this approach was only done for 70 of 87 MPs. After generation of the list of suspect OTPs, Approach 2 was applied. However, strictly following Approach 1 would also enable the identification of OTPs present in WWTPs.

Within Approach 2, OTP signals were identified that were simultaneously formed in the *O3bAll* experiments (for all 87 MPs) and the WWTPs. A re-measurement of *O3bMix* samples together with the WWTP samples was necessary to acquire MS<sup>2</sup> scans on all identified OTP masses and to assign them to their corresponding parent MPs.

### 2.5.1. Generation of a list of suspect OTPs using laboratory ozonation batch experiments (*O3bMix*) in Approach 1 (A–C)

For the identification of OTP signals in laboratory batch experiments, we further developed the method from Gulde et al. (2016) by using the software Compound Discoverer 2.1 (Thermo Scientific). OTP signals were identified for each parent MP and separately for positive and negative ionization mode. To do so, the samples of the two mixtures, in which the respective MP was spiked, and the sample of another mixture, where no structurally related MP was spiked (used as control), were uploaded. To identify likely OTP signals, a non-target approach (i.e., without previous knowledge or expectation of, e.g., OTP masses) was used on these *O3bMix* samples by applying the following automatic and manual filter criteria: (i) a minimal five-fold increase in peak area for the ozonated samples compared to the non-ozonated samples; (ii) presence in both mixtures containing the respective MP; (iii) absence in the control mixture; and (iv) reasonable peak shape (for details, see Text S4.1, Figs. S10–13, and Table S5, SI). In general, the goal of this evaluation was to get a complete list, while accepting a certain number of false positives, since confirmation of the signal being a relevant OTP followed only after its detection in WWTP samples. Therefore, also no component (i.e., isotope and/or adduct) grouping was performed at this stage.

### 2.5.2. Identification and confirmation of OTP signals in WWTP samples using Approach 2

To identify OTP signals that were formed in our reference laboratory ozonation batch experiment (*O3bAll*) and in the WWTPs, we used Compound Discoverer 2.1 (Thermo Scientific) for a separate evaluation in positive and negative mode. We uploaded the samples from the *O3bAll* experiments and from the four different WWTPs. For signal identification, an automatic filter and a manual selection was applied. The automatic filter had the following criteria: (i) presence of a signal in at least one *O3bAll* sample after ozone addition; (ii) a minimal two-fold increase in peak area in the

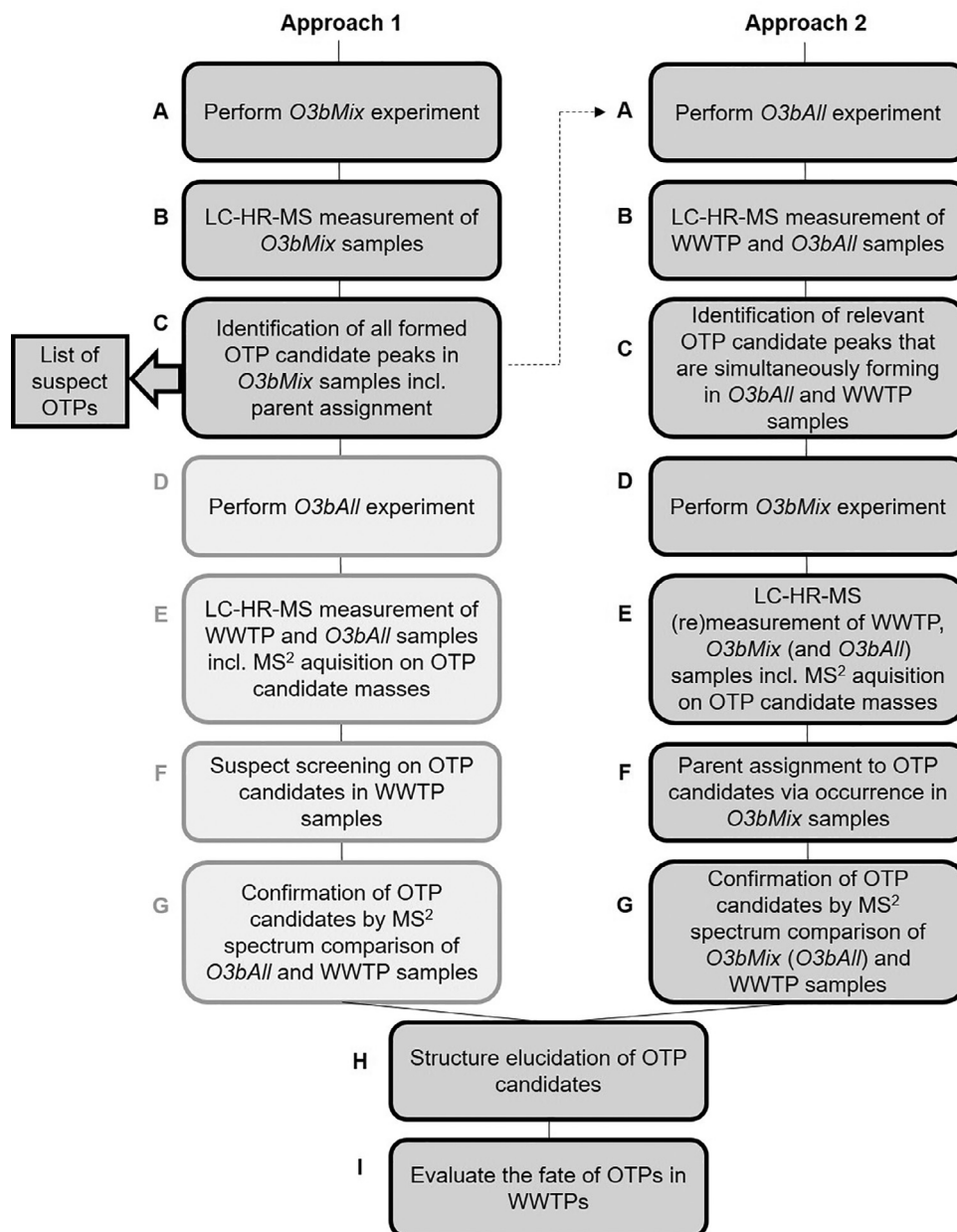


**Fig. 1.** Two possible approaches to identify OTPs in WWTPs: Approach 1 was only followed until the generation of a list of suspect OTPs (A-C) and Approach 2 was taken further. However, the light grey boxes show which steps would be necessary to complete Approach 1.

*O3bAll* experiment for the ozonated samples compared to the non-ozonated samples; (iii) a minimal five-fold increase in peak area in the *O3bAll* samples compared to the blank samples (20 mL nanopure water spiked with 16  $\mu$ L ISTD stock solution); (iv) peak retention time between 4 and 28 min; and (v) a maximal peak area of at least 10000 / 1000 in positive / negative mode (for details, see Text S4.2, Figs. S14-16, and Table S6, SI). Signals were manually selected based on their pattern over time in the ozonation batch experiments and their occurrence in the WWTP samples. Since we had knowledge of suspect OTPs of 70 MPs from Approach 1, we used this information by uploading the list of all exact masses of the identified OTP signals. That way, an easier selection of matching OTP signals was possible, since MS<sup>2</sup> spectra were available. However, Approach 2 can be applied without this prior knowledge.

For the parent MP assignment, as well as for the confirmation of identified OTP signals in the WWTP samples, a sample of each of the 19 *O3bMix* experiments, the *O3bAll* samples, and an OZO

sample of all WWTP campaigns were re-measured for MS<sup>2</sup> spectra acquisition for all OTPs of the 87 MPs; the samples were then uploaded into Compound Discoverer 2.1. The assignment of OTPs to their respective parent MPs was achieved by examining which parent MP was spiked into the *O3bMix* experiments in which the OTP signal was observed.

For confirmation of the OTP signal, a clean MS<sup>2</sup> spectrum of the *O3bMix* or *O3bAll* samples was manually selected as a reference spectrum. Afterwards, the reference MS<sup>2</sup> spectrum was compared to the highest acquired MS<sup>2</sup> spectrum for the respective mass of each WWTP OZO sample. Similarity of the MS<sup>2</sup> spectra were calculated using the modified cosine or dot product using the *MSMSim* package (Schollée 2017). Weighting factors for *m/z* and intensity were 0 and 0.75, respectively; further details are available in Schollée et al. (2017). Generally, the better the agreement between the MS<sup>2</sup> spectra, the closer are the scores to 1.0. The scores were categorized in the following five groups by visual inspection

of MS<sup>2</sup> spectra of known compounds: 1.0–0.6 very good (+++), 0.6–0.4 good (++), 0.4–0.2 ok (+), 0.2–0.1 bad (–), and 0.1–0.0 very bad (–). All values >0.2 were treated as sufficient. The MS<sup>2</sup> spectra match of the whole OTP was classified as sufficient if >40% of all MS<sup>2</sup> scores of OZO samples, for which a signal was detected, were rated as sufficient (>0.2).

## 2.6. Structure elucidation of OTPs

Multiple components of an OTP, e.g., different adducts (also in both modes) or in-source fragments, could be identified as OTP signals by our approaches. Therefore, related signals were grouped manually by comparing RTs and peak shapes within Compound Discoverer 2.1. Assumed adducts, e.g., [M+H]<sup>+</sup>, [M-H]<sup>–</sup>, or [M+FA-H]<sup>–</sup>, were assigned and chemical formulas were proposed using Xcalibur QualBrowser 4.1 (Thermo Scientific). Based on the MS<sup>2</sup> spectra and on known ozonation reaction pathways, plausible OTP structures were proposed either using Compound Discoverer 2.1 or by visual interpretation. Confidence levels were assigned as proposed by Schymanski et al. (2014).

## 2.7. Evaluation of the fate of the OTPs in the WWTPs

To investigate the fate of the identified OTPs during ozonation and the different WWTP post-treatment steps, the peak areas (as calculated by Compound Discoverer 2.1) were used. The percent difference between the WWTP samples BIO and OZO or between the WWTP samples OZO and EFF were calculated as  $\frac{\text{area}_{\text{BIO}} - \text{area}_{\text{OZO}}}{\max(\text{area}_{\text{BIO}}, \text{area}_{\text{OZO}})} \times 100$  or  $\frac{\text{area}_{\text{OZO}} - \text{area}_{\text{EFF}}}{\max(\text{area}_{\text{OZO}}, \text{area}_{\text{EFF}})} \times 100$ , respectively. Signals were defined as predominately forming during the ozonation step of the WWTPs if their relative difference between BIO and OZO samples was <–33% in ≥50% of the WWTP samples. Only these signals were used for further analyses. To evaluate the fate in the different WWTP post-treatment steps, a classification of relative differences was introduced (see Section 3.3.4).

## 3. Results and discussion

### 3.1. Ozonation conditions of the laboratory ozonation batch experiments

OTP identification is simplified if experimental solutions are free of DOM. However, the ozonation conditions, i.e., ozone exposure, •OH exposure, and R<sub>ct</sub> value, are controlled by complicated interactions between O<sub>3</sub>/•OH with DOM (Elovitz and von Gunten 1999, Elovitz et al. 2000, von Sonntag and von Gunten 2012). To overcome the inherent problems of DOM for the chemical analysis of OTPs, the ozone-relevant properties of DOM were simulated by methanol and acetate as promoter and inhibitor, respectively, thereby adjusting the ozone and •OH exposures to values similar to real water matrices (see Text S2.1 for details). The resulting ozone exposures were 0.011±0.003 Ms in the O3bMix experiments (note that the samples of all 19 experiments reacted to complete ozone depletion due to problems with ozone quenching) and in the O3bAll experiment 0.00048, 0.0024, 0.0058, 0.0071, and 0.023 Ms in the samples at 45 s, 150 s, 300 s, 480 s, and at full ozone depletion, respectively. These results are in the range of ozone exposures determined for nine different municipal wastewaters (Lee et al. 2013), which were reported to be 0.0002–0.0028 Ms for a specific ozone dose of 0.5 gO<sub>3</sub>/gDOC and 0.004–0.013 Ms for a specific ozone dose of 1 gO<sub>3</sub>/gDOC. Also, the ozone exposures of 0.0015–0.024 Ms determined by Elovitz et al. (2000) for five lake and two river waters with specific ozone doses of 0.67–1.0 gO<sub>3</sub>/gDOC were in the same range. The estimated average R<sub>ct</sub> value for the O3bMix experiments was (2.3±0.7) × 10<sup>–8</sup> and for the O3bAll experiments 1.4 × 10<sup>–8</sup>, which is in a similar range as

for nine municipal wastewater effluents (2.2 × 10<sup>–8</sup>–19 × 10<sup>–8</sup>) (Lee et al. 2013) and seven surface waters (0.12 × 10<sup>–8</sup>–5.8 × 10<sup>–8</sup>) (Elovitz et al. 2000). Overall, the ozonation conditions in the simulated water matrix were similar to those in municipal wastewater effluents and surface waters, indicating that the simulated water matrices were representative of real water matrices. Furthermore, the good agreement between the observed and predicted abatement of four MPs (from experimentally determined second-order rate constants for their reactions with ozone and •OH radicals (see Text S5 and Fig. S17, SI)) confirms the significance of such batch experiments.

### 3.2. Detected suspect OTPs using laboratory ozonation batch experiments (O3bMix) in Approach 1 (A–C)

The 87 MPs were divided into 19 smart mixtures for individual ozonation batch experiments (O3bMix). The distribution in mixtures significantly reduced the number of batch experiments needed to relate the OTPs to the corresponding parent MPs. A list of suspect OTPs was generated by identification of signals that were formed in the O3bMix experiments for each parent MP. The 70 selected parent MPs, which are expected to occur in the highest concentrations in wastewater (Bourgin et al. 2018), resulted in 1749 OTP signals. These OTP signals are listed in Table S2 (SI) and were identified in positive (777) and negative (972) modes. Different components (e.g., isotopes, adducts, in-source fragments) were not grouped together, since a rather comprehensive list is beneficial for a subsequent screening in WWTP samples.

For our final identification of OTPs in WWTPs, Approach 2 was taken (see Section 3.3). However, the list generated with Approach 1 was also consulted and can be used in other studies to screen for potential OTPs.

### 3.3. Results from ozonated WWTPs samples

#### 3.3.1. Identification of OTPs in ozonated samples from WWTPs

The samples of four WWTPs were screened for the 87 selected parent MPs and for OTPs formed from them that had matching signals in the ozonation batch experiments (O3bAll, containing all MPs), as described in Approach 2 in Fig. 1. In the WWTP Neugut, the full-scale ozonation (0.5 gO<sub>3</sub>/gDOC) was followed by sand filtration (SF), while the other three WWTPs operated pilot plants with a pre-ozonation (0.21–0.33 gO<sub>3</sub>/gDOC) followed by activated carbon treatment. Different numbers of MPs (from the selected 87 MPs) were abundant in the samples after biological treatment (BIO) in the different WWTPs: 71–73 in Neugut, 64–68 in Glarnerland, 59 in Altenrhein, and 63 in ProReno (concentrations are provided in Table S1 and Text S6, SI). MPs found in the highest average concentrations of >1 µg/L were acesulfame, metformin, sucralose, and 2,7-naphthalic disulfonic acid.

In total, 153 OTP signals matching with signals formed in the O3bAll samples were detected in the WWTP samples (Table S3, SI). After grouping component signals together and filtering for signals that were predominantly formed during the ozonation step, 84 OTPs remained, which originated from 40 of the 87 investigated MPs. Of the 47 MPs for which no OTP was assigned, 15 MPs were not detected or detected in BIO with average concentrations < 10 ng/L and 19 MPs < 50 ng/L. No OTPs were assigned to atenolol acid and valsartan acid, however, their OTPs could be the same as for atenolol and valsartan. Four MPs occurring in higher concentrations in BIO with no OTP assigned were poorly abated, on average by <30%, during ozonation (2,7-naphthalic disulfonic acid, acesulfame, levetiracetam, and metformin) and two MPs by 40–50% (4/5-methylbenzotriazole and benzotriazole). These are MPs known to exhibit low reactivity with ozone at the pH of the wastewater effluents (Bourgin et al. 2018, Lee et al. 2014, Mathon et al. 2021).



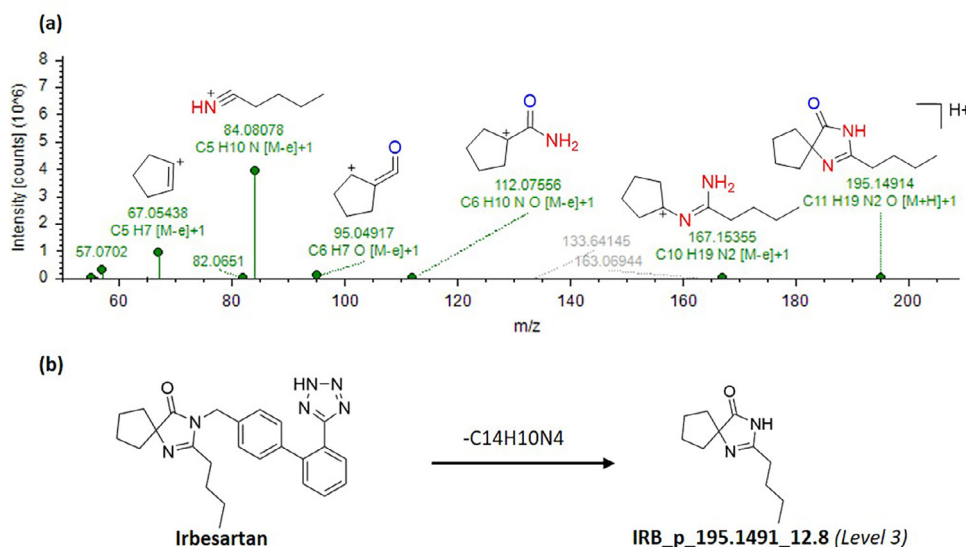


Fig. 2. Structure elucidation of an OTP of irbesartan: (a) MS<sup>2</sup> spectrum and (b) structure of the parent irbesartan and proposed structure of OTP IRB\_p\_195.1491\_12.8.

Between 1 and 7 of the detected 84 OTPs were assigned to the same parent MPs (Fig. S18 and Text S6, SI). For most parents (22), only 1 OTP was found, for 17 MPs 2–4 OTPs, while 6 OTPs were observed for carbamazepine and 7 OTPs for sitagliptin.

From the 84 OTPs, 22 were not found in the evaluation of the *O3bMix* samples in Approach 1. Ten of them were assigned to six parent MPs which were not evaluated (only 70 of all 87 MPs expected to occur in the highest concentrations in wastewater were screened in Approach 1 due to time constraints). The other 12 OTPs may be fast-reacting OTPs, since the *O3bMix* samples reacted until full ozone depletion and fast-forming OTPs, which further degraded at higher ozone exposure, were most likely abated again and hence not identified in these samples. Moreover, OTPs with less intense signals might be found by Approach 2, since the *O3bAll* samples (measured with online-SPE enrichment) were concentrated by a factor of 2–5 compared to *O3bMix* samples in Approach 1.

### 3.3.2. Chemical structure of identified OTPs in WWTPs

The structures of 84 OTPs were elucidated. Figs. 2 and 3 show the available data exemplarily for OTP IRB\_p\_195.1491\_12.8 (details for all OTPs in Table S3, Text S6, and Fig. S19, SI). Table 1 summarizes the most relevant data for all 84 OTPs (OTP name, parent MP, adduct, formula, confidence level, reference, evaluation of the MS<sup>2</sup> match of the OZO WWTP samples to the ozonation batch sample, fate of OTPs in the different WWTPs, and proposed structure).

OTP IRB\_p\_195.1491\_12.8 was detected in positive mode at a measured  $m/z$  195.1491 and RT 12.8 min (Fig. 2). Since it was present in the *O3bMix* samples where irbesartan was spiked, it was assigned to this MP. The formula C<sub>11</sub>H<sub>18</sub>ON<sub>2</sub>+H<sup>+</sup> fit best to the measured mass ( $\Delta$ ppm -0.31). A modification of -C<sub>14</sub>H<sub>10</sub>N<sub>4</sub> between the parent irbesartan (C<sub>25</sub>H<sub>28</sub>N<sub>6</sub>O) and this OTP likely results from a cleavage of the tetrazolebiphenylmethyl moiety, which was also detected as an OTP (sartans\_p\_251.0924\_17.9). This moiety is common for all sartans and its cleavage was also observed for candesartan (CAN\_p\_207.0766\_17.0) and valsartan (VAL\_n\_200.1289\_18.1). The MS<sup>2</sup> spectrum of RB\_p\_195.1491\_12.8 is shown in Fig. 2a and is publicly available on MassBank, together with all available spectra of the other OTPs (MassBank 2006). For the structure elucidation, MS<sup>2</sup> fragments were annotated by Compound Discoverer 2.1 and compared with the measured fragments. The predicted structures of the MS<sup>2</sup> fragments are drawn

above the fragments. Highlighted in green are measured MS<sup>2</sup> fragments that can be explained by predicted fragments for the proposed structure, showing a fit for all relevant fragments for IRB\_p\_195.1491\_12.8. The proposed structure (Fig. 2b) was assigned a confidence level 3 according to Schymanski et al. (2014). The MS<sup>2</sup> fragments and neutral losses of other OTPs were also manually annotated, if the Compound Discoverer 2.1 annotation was not sufficient.

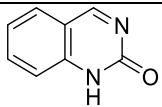
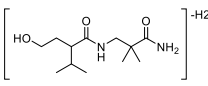
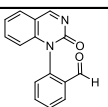
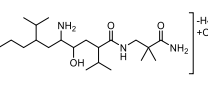
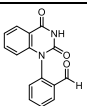
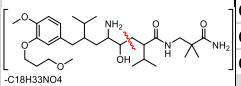
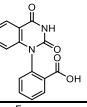
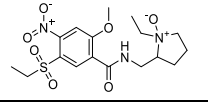
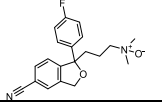
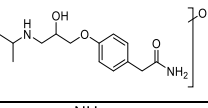
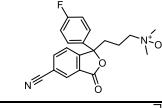
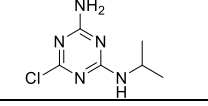
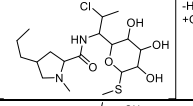
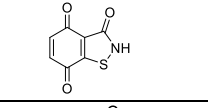
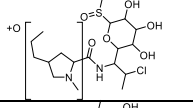
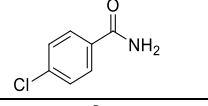
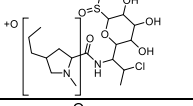
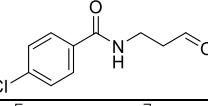
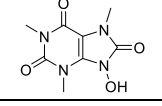
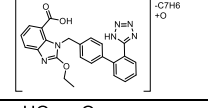
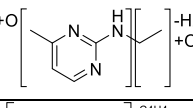
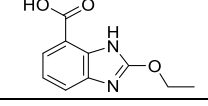
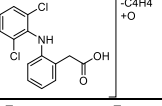
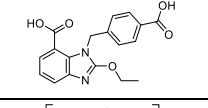
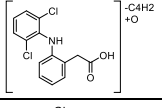
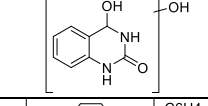
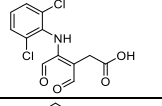
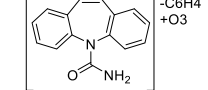
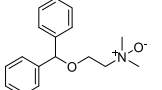
From the 84 identified and structure-elucidated OTPs, 6 were assigned with level 1 (confirmed structure by reference standard), 6 with level 2a (probable structure by library spectrum match), 71 with level 3 (tentative candidate structure) and one with level 5 (exact mass). The OTP without structure assignment (nk\_n\_293.1148\_16.2) will not be further discussed below.

Only 35 (42%) of the remaining 83 OTPs with proposed structure from 40 MPs were previously reported in literature (Table 1 and Text S6, SI). OTPs of 20 MPs have, to the best of our knowledge, not been previously described, and for 8 MPs, additional, novel OTPs were observed. However, we did not find all OTPs that were proposed in literature. For diclofenac, for example, diclofenac 2,5-quinone imine was reported elsewhere as a major OTP (Coelho et al. 2009, El-taliawy et al. 2018, Faber et al. 2014, Sein et al. 2008). We saw a signal for this OTP in some wastewater samples, however, it was not present in our batch experiments and was therefore not discovered with our workflow.

Cleavage of part of the molecule was observed for more than half of the parent MPs (52), 14 of which were *N*-dealkylations, a well-known ozone reaction (Lim et al. 2019). Nearly all cleavages co-occurred with an oxidation. The following atomic modifications of the OTP relative to its parent were observed: plus one oxygen (+O), minus two hydrogens plus one oxygen (-H<sub>2</sub>+O), minus two hydrogens plus two oxygens (-H<sub>2</sub>+O<sub>2</sub>), minus two hydrogens (-H<sub>2</sub>), or a combination thereof. A modification of (+O) can occur through the formation of an *N*-oxide, an *S*-oxide or a hydroxylation. *N*-oxides were found in 13 OTPs (7 OTPs with only this modification). Their formation from MPs with tertiary amine functional groups is well-known and has been detected in wastewater previously (Bollmann et al. 2016, Bourgin et al. 2018, Hörsing et al. 2012, Knopp et al. 2016, Lajeunesse et al. 2013, Lester et al. 2013, Lim et al. 2019, Merel et al. 2017, Zimmermann et al. 2012, Zucker et al. 2018). *N*-oxides of amisulpride, citalopram, clindamycin, diphenhydramine,

**Table 1**

The detected 84 OTPs with their proposed structures. The OTPs are ordered alphabetically according to the abbreviation of their parent compounds. The following information is provided in the top left cell: OTP name; parent name; formula; (a-g) fate defined as (A) *abatement*, (S) *stable*, or (F) *formation* in the following post-treatments: (a) SFa, (b) SFb, (c) GAC1a, (d) GAC1b, (e) GAC1c, (f) GAC2, (g) PAC; (h) assumed adduct; (i) reference, if available; (j) confidence level (Schymanski et al. 2014); (k) evaluation, if MS<sup>2</sup> spectra match was sufficient as yes (y) or no (n); proposed structure. For more detailed information for each OTP see Text S6, SI.

|                     |       |   |                     |        |   |   |   |   |   |   |   |   |   |   |   |   |   |
|---------------------|-------|---|---------------------|--------|---|---|---|---|---|---|---|---|---|---|---|---|---|
| OTP name            | h     | proposed structure  | CBZ_p_147.0552_14.3 | m+H+   |    |   |   |   |   |   |   |   |   |   |   |   |   |
| parent              | i     |   | Carbamazepine       | 8      |   |   |   |   |   |   |   |   |   |   |   |   |   |
| formula             | j     |   | C8H6ON2             | 3      |   |   |   |   |   |   |   |   |   |   |   |   |   |
| a                   | b     |   | c                   | d      |   | e | f | g | k | S | S | S | S | S | S | A | y |
| ALI_n_241.1556_15.2 | m-H-  |    | CBZ_p_251.0812_17.9 | m+H+   |    |   |   |   |   |   |   |   |   |   |   |   |   |
| Aliskiren           |       |   | Carbamazepine       | 8-10   |   |   |   |   |   |   |   |   |   |   |   |   |   |
| C12H22O3N2          | 3     |   | C15H10O2N2          | 2a     |   |   |   |   |   |   |   |   |   |   |   |   |   |
| S                   | S     |   | S                   | S      |   | S | S | S | A | n | A | S | A | A | A | A | A |
| ALI_n_428.2762_19.1 | m-H-  |    | CBZ_p_267.0762_17.7 | m+H+   |    |   |   |   |   |   |   |   |   |   |   |   |   |
| Aliskiren           |       |   | Carbamazepine       | 8-10   |   |   |   |   |   |   |   |   |   |   |   |   |   |
| C21H39O6N3          | 3     |   | C15H10O3N2          | 2a     |   |   |   |   |   |   |   |   |   |   |   |   |   |
| S                   | S     |   |                     |        |   |   |   |   |   | n | F | S |   | S | S | S | A |
| ALI_p_225.1597_15.3 | m+H+  |    | CBZ_p_283.0711_17.3 | m+H+   |    |   |   |   |   |   |   |   |   |   |   |   |   |
| Aliskiren           |       |   | Carbamazepine       | 8-10   |   |   |   |   |   |   |   |   |   |   |   |   |   |
| C12H20O2N2          | 3     |   | C15H10O4N2          | 2a     |   |   |   |   |   |   |   |   |   |   |   |   |   |
| S                   | S     |   | S                   | S      |   | S | S | S | A | y | F | F | F | F | F | F | F |
| ASP_p_416.1486_12.8 | m+H+  |    | CIT_p_341.1661_16.2 | m+H+   |    |   |   |   |   |   |   |   |   |   |   |   |   |
| Amisulpride         |       |   | Citalopram          | 11, 12 |   |   |   |   |   |   |   |   |   |   |   |   |   |
| C17H25O7N3S         | 3     |   | C20H21O2N2F         | 1      |   |   |   |   |   |   |   |   |   |   |   |   |   |
| S                   | S     |   |                     |        |   |   |   |   |   | y | S | S | A | A | A | S | A |
| ATE_p_283.1666_21.2 | m+H+  |    | CIT_p_355.1451_15.9 | m+H+   |    |   |   |   |   |   |   |   |   |   |   |   |   |
| Atenolol            | 1-3   |   | Citalopram          |        |   |   |   |   |   |   |   |   |   |   |   |   |   |
| C14H22O4N2          | 3     |   | C20H19O3N2F         | 3      |   |   |   |   |   |   |   |   |   |   |   |   |   |
| S                   | S     |   | S                   | S      |   | S | S | F | S | y | S | S | A | A |   | S | A |
| ATZ_p_188.0697_16.8 | m+H+  |   | CLI_n_453.1466_17.7 | m-H-   |   |   |   |   |   |   |   |   |   |   |   |   |   |
| Atrazine            | 4-6   |   | Clindamycin         |        |   |   |   |   |   |   |   |   |   |   |   |   |   |
| C6H10N5Cl           | 3     |   | C18H31O7N2ClS       | 3      |   |   |   |   |   |   |   |   |   |   |   |   |   |
| S                   | S     |   |                     |        |   |   |   |   |   | y | S | S | S | S | S | S | A |
| BIT_n_215.9525_17.0 | m+Cl- |  | CLI_p_457.1769_14.7 | m+H+   |  |   |   |   |   |   |   |   |   |   |   |   |   |
| Benzisothiazolone   |       |   | Clindamycin         |        |   |   |   |   |   |   |   |   |   |   |   |   |   |
| C7H3O3NS            | 3     |   | C18H33O7N2ClS       | 3      |   |   |   |   |   |   |   |   |   |   |   |   |   |
| S                   | S     |   | A                   | A      |   |   |   |   |   | y | S | S | S | S | S | F | A |
| BZF_p_156.0209_16.9 | m+H+  |  | CLI_p_457.1769_15.1 | m+H+   |  |   |   |   |   |   |   |   |   |   |   |   |   |
| Bezafibrate         | 7     |   | Clindamycin         |        |   |   |   |   |   |   |   |   |   |   |   |   |   |
| C7H6ONCl            | 3     |   | C18H33O7N2ClS       | 3      |   |   |   |   |   |   |   |   |   |   |   |   |   |
| S                   | A     |   | A                   | A      |   | A | A | A | A | n | S | S | A | A | S | S | A |
| BZF_p_212.0469_17.1 | m+H+  |  | COF_n_225.0627_12.2 | m-H-   |  |   |   |   |   |   |   |   |   |   |   |   |   |
| Bezafibrate         |       |   | Caffeine            | 13     |   |   |   |   |   |   |   |   |   |   |   |   |   |
| C10H10O2NCl         | 3     |   | C8H10O4N4           | 3      |   |   |   |   |   |   |   |   |   |   |   |   |   |
| S                   | S     |   |                     |        |   |   |   |   |   | n | S | S | S | S | S | S | S |
| CAN_n_365.1000_18.9 | m-H-  |  | CYP_p_168.0767_12.4 | m+H+   |  |   |   |   |   |   |   |   |   |   |   |   |   |
| Candesartan         |       |   | Cyprodinil          |        |   |   |   |   |   |   |   |   |   |   |   |   |   |
| C17H14O4N6          | 3     |   | C7H9O2N3            | 3      |   |   |   |   |   |   |   |   |   |   |   |   |   |
| S                   | F     |   | A                   | A      |   |   |   |   |   | n | S | S | S | A | S | S | A |
| CAN_p_207.0766_17.0 | m+H+  |  | DIC_n_257.9729_16.7 | m-H-   |  |   |   |   |   |   |   |   |   |   |   |   |   |
| Candesartan         |       |   | Diclofenac          |        |   |   |   |   |   |   |   |   |   |   |   |   |   |
| C10H10O3N2          | 3     |   | C10H7O3NCl2         | 3      |   |   |   |   |   |   |   |   |   |   |   |   |   |
| S                   | S     |   | S                   | S      |   | S | F | F | F | F | S | y | S | F | F | F | F |
| CAN_p_341.1130_19.6 | m+H+  |  | DIC_n_259.9873_15.6 | m-H-   |  |   |   |   |   |   |   |   |   |   |   |   |   |
| Candesartan         |       |   | Diclofenac          |        |   |   |   |   |   |   |   |   |   |   |   |   |   |
| C18H16O5N2          | 3     |   | C10H9O3NCl2         | 3      |   |   |   |   |   |   |   |   |   |   |   |   |   |
| S                   | F     |   | F                   |        |   |   |   |   |   | n | S | S | S |   | F | A | n |
| CBZ_n_179.0461_17.2 | m-H-  |  | DIC_n_299.9834_16.4 | m-H-   |  |   |   |   |   |   |   |   |   |   |   |   |   |
| Carbamazepine       | 8     |   | Diclofenac          |        |   |   |   |   |   |   |   |   |   |   |   |   |   |
| C8H8O3N2            | 3     |   | C12H9O4NCl2         | 3      |   |   |   |   |   |   |   |   |   |   |   |   |   |
| S                   | A     |   | A                   | S      |   |   |   |   |   | n | F | S | S | S | S | S | S |
| CBZ_n_207.0409_17.6 | m-H-  |  | DIP_p_272.1644_16.5 | m+H+   |  |   |   |   |   |   |   |   |   |   |   |   |   |
| Carbamazepine       |       |   | Diphenhydramine     | 12     |   |   |   |   |   |   |   |   |   |   |   |   |   |
| C9H8O4N2            | 3     |   | C17H21O2N           | 2a     |   |   |   |   |   |   |   |   |   |   |   |   |   |
| S                   | S     |   | A                   | A      |   | A | A | A | A | A | S | S | A | A | A | S | A |

(continued on next page)

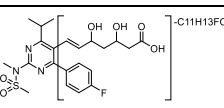
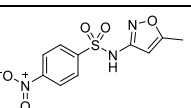
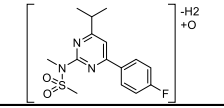
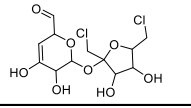
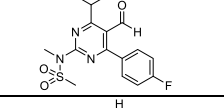
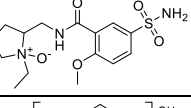
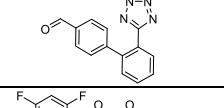
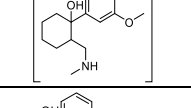
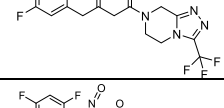
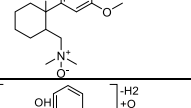
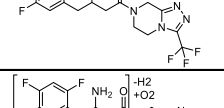
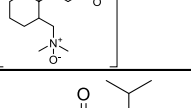
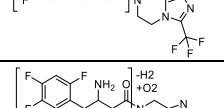
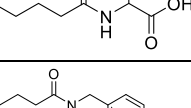
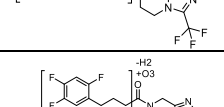
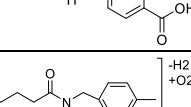
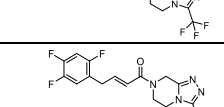
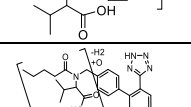
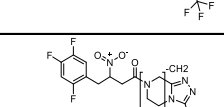
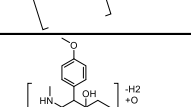
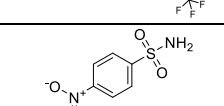
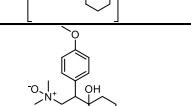
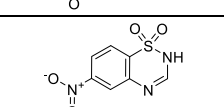
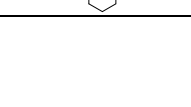
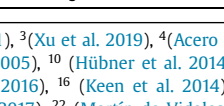


Table 1 (continued)

|                      |         |  |                     |        |    |
|----------------------|---------|--|---------------------|--------|----|
| DIU_p_215.0582_14.8  | m+H+    |  | IRB_p_329.1858_19.4 | m+H+   |    |
| Diuron               | 14      |  | Irbesartan          |        |    |
| C9H11O2N2Cl          | 3       |  | C19H24O3N2          | 3      |    |
|                      | y       |  | F S S S S S S A     | y      |    |
| DMT_p_246.1489_17.5  | m+H+    |  | LAM_p_259.9988_13.7 | m+H+   |    |
| N-Desmethyltramadol  |         |  | Lamotrigine         | 16     |    |
| C15H19O2N            | 3       |  | C9H7O2N3Cl2         | 3      |    |
| S S F A A            | n       |  | S S A S A           | y      |    |
| ETO_n_302.1395_19.6  | m-H-    |  | LID_n_192.0665_16.0 | m-H-   |    |
| Etodolac             |         |  | Lidocaine           |        |    |
| C17H21O4N            | 3       |  | C10H11O3N           | 3      |    |
| S S S S S S A        | y       |  | F F F A A           | n      |    |
| FAD_n_232.0224_21.7  | m-H-    |  | LID_p_247.1438_17.8 | m+H+   |    |
| Flufenamic acid      |         |  | Lidocaine           |        |    |
| C9H6O3NF3            | 3       |  | C14H18O2N2          | 3      |    |
| A A A A A            | y       |  | S A A F F A         | y      |    |
| FAD_n_258.0384_19.6  | m-H-    |  | LID_p_251.1752_13.6 | m+H+   |    |
| Flufenamic acid      |         |  | Lidocaine           | 12     |    |
| C11H8O3NF3           | 3       |  | C14H22O2N2          | 1      |    |
| A A A A A A          | y       |  | S S A A S S A       | y      |    |
| FAD_n_260.0537_19.0  | m-H-    |  | LID_p_265.1545_12.4 | m+H+   |    |
| Flufenamic acid      |         |  | Lidocaine           |        |    |
| C11H10O3NF3          | 3       |  | C14H20O3N2          | 3      |    |
| F A A                | n       |  | S S F A A A A S     | y      |    |
| FEN_p_290.2478_18.3  | m+H+    |  | LVI_n_271.0392_15.1 | m-H-   |    |
| Fenpropidin          |         |  | Levamisole          |        |    |
| C19H31ON             | 3       |  | C10H12O5N2S         | 3      |    |
|                      | A y     |  | S S                 | A y    |    |
| FEN_p_320.2220_22.5  | m+H+    |  | MAA_n_250.0719_18.5 | m-H-   |    |
| Fenpropidin          |         |  | Mefenamic acid      |        |    |
| C19H29O3N            | 3       |  | C12H13O5N           | 3      |    |
| F                    | S n     |  | S S S A F           | n      |    |
| FFA_n_189.0167_20.1  | m-H-    |  | nk_n_293.1148_16.2  | NA     | NA |
| Fenfluramine         |         |  | NA                  |        |    |
| C8H5O2F3             | 3       |  | NA                  | 5      |    |
|                      | A F A y |  | S S                 | A y    |    |
| FLE_n_362.04655_19.2 | m+FA-H- |  | OXA_p_285.0423_21.9 | m+H+   |    |
| Flecainide           |         |  | Oxazepam            |        |    |
| C11H9O3NF6           | 3       |  | C15H9O2N2Cl         | 3      |    |
|                      | S n     |  | S S A S S A         | y      |    |
| FLE_n_374.0465_19.4  | m-H-    |  | PHE_p_137.0709_12.9 | m+H+   |    |
| Flecaicid            |         |  | Phenazone           |        |    |
| C13H11O5NF6          | 3       |  | C7H8ON2             | 3      |    |
| F                    | A n     |  | S S A A A S A       | y      |    |
| GAB_p_186.1124_17.5  | m+H+    |  | PHE_p_137.0709_14.1 | m+H+   |    |
| Gabapentin           |         |  | Phenazone           |        |    |
| C9H15O3N             | 3       |  | C7H8ON2             | 3      |    |
| S S A F F A          | y       |  | S S A A A A A       | y      |    |
| HCT_n_293.9415_10.8  | m-H-    |  | PHE_p_165.1021_17.6 | m+H+   |    |
| Hydrochlorothiazide  | 15      |  | Phenazone           | 17, 18 |    |
| C7H6O4N3ClS2         | 1       |  | C9H12ON2            | 3      |    |
| S S A A S S A        | y       |  | S S S S S F A       | y      |    |
| IRB_p_195.1491_12.8  | m+H+    |  | PHE_p_237.0868_15.1 | m+H+   |    |
| Irbesartan           |         |  | Propylamide         |        |    |
| C11H18ON2            | 3       |  | C11H12O4N2          | 3      |    |
| S S S S S S A        | y       |  | S S S F F F S       | y      |    |
| IRB_p_253.1545_14.2  | m+H+    |  | PYZ_n_301.9991_22.6 | m-H-   |    |
| Irbesartan           |         |  | Propylamide         |        |    |
| C13H20O3N2           | 3       |  | C12H11O4NCl2        | 3      |    |
| S S S S S S y        |         |  | S                   | n      |    |

(continued on next page)

Table 1 (continued)

|                            |         |   |                     |           |   |
|----------------------------|---------|---|---------------------|-----------|---|
| ROS_n_300.0656_17.7        | m-H-    |    | SMX_n_282.0188_18.0 | m-H-      |    |
| Rosuvastatin               |         |   | Sulfamethoxazole    | 21, 23-26 |   |
| C11H15O5N3S                | 3       |   | C10H9O5N3S          | 3         |   |
| A S                        | n       |   | S S A A A A y       |           |   |
| ROS_n_336.0821_20.7        | m-H-    |    | SUC_n_403.0202_13.3 | m+FA-H-   |    |
| Rosuvastatin               |         |   | Sucralose           | 27        |   |
| C15H16O3N3FS               | 3       |   | C12H16O8Cl2         | 3         |   |
| S S A                      | F A n   |   | S F A S S S A y     |           |   |
| ROS_p_352.1124_22.0        | m+H+    |    | SUL_p_358.1432_10.5 | m+H+      |    |
| Rosuvastatin               |         |   | Sulpiride           | 12, 28    |   |
| C16H18O3N3FS               | 3       |   | C15H23O5N3S         | 1         |   |
| S S A A A A A y            |         |   | S S A A S S A y     |           |   |
| Sartans_p_251.0924_17.9    | m+H+    |    | TRA_p_266.1749_12.8 | m+H+      |    |
| Sartans                    | 19      |   | Tramadol            |           |   |
| C14H10O4N                  |         |   | C15H23O3N           | 3         |   |
| S S S                      | A S A y |   | S S                 | A n       |   |
| SIT_n_405.0789_18.6        | m-H-    |    | TRA_p_280.1905_14.4 | m+H+      |    |
| Sitagliptin                | 20      |   | Tramadol            | 12, 29    |   |
| C16H12O2N4F6               | 2a      |   | C16H25O3N           | 1         |   |
| S S                        | A A n   |   | S S S S A S A y     |           |   |
| SIT_n_420.0899_18.2        | m-H-    |    | TRA_p_294.1699_11.0 | m+H+      |    |
| Sitagliptin                | 20      |   | Tramadol            |           |   |
| C16H13O2N5F6               | 3       |   | C16H23NO4           | 3         |   |
| S S A A S A A n            |         |   | F S F A F y         |           |   |
| SIT_n_436.0847_18.3        | m-H-    |   | VAL_n_200.1289_18.1 | m-H-      |   |
| Sitagliptin                | 20      |   | Valsartan           | 19        |   |
| C16H13O3N5F6               | 3       |   | C10H19O3N           | 2a        |   |
| S S                        | n       |   | A F F S A A n       |           |   |
| SIT_n_436.0847_19.2        | m-H-    |  | VAL_n_234.1133_17.8 | m-H-      |  |
| Sitagliptin                | 20      |   | Valsartan           | 19        |   |
| C16H13O3N5F6               | 3       |   | C13H17O3N           | 2a        |   |
| S S                        | A n     |   | S S A A A n         |           |   |
| SIT_n_437.0687_20.7        | m-H-    |  | VAL_n_334.1657_20.4 | m-H-      |  |
| Sitagliptin                | 20      |   | Valsartan           | 19        |   |
| C16H12O4N4F6               | 3       |   | C18H25O5N           | 3         |   |
| S S A A A A A y            |         |   | S S A S F F n       |           |   |
| SIT_p_391.0988_19.8        | m+H+    |  | VAL_p_450.2132_19.2 | m+H+      |  |
| Sitagliptin                | 20      |   | Valsartan           | 19        |   |
| C16H12ON4F6                | 3       |   | C24H27N5O4          | 3         |   |
| S S A                      | A y     |   | S S A S A S A y     |           |   |
| SIT_p_426.0996_19.1        | m+H+    |  | VEN_p_278.1749_19.4 | m+H+      |  |
| Sitagliptin                | 20      |   | Venlafaxine         |           |   |
| C15H13O3N5F6               | 3       |   | C16H23NO3           | 3         |   |
| S F                        | A y     |   | S S                 | A y       |   |
| SMX/SMZ_n_200.9972_14.1    | m-H-    |  | VEN_p_294.2064_16.1 | m+H+      |  |
| Sulfameth-oxazole / -azine |         |   | Venlafaxine         | 12, 30-32 |   |
| C6H6O4N2S                  | 3       |   | C17H27NO3           | 1         |   |
| S S                        | A A y   |   | S S S A S S A y     |           |   |
| SMX_n_225.9926_16.4        | m-H-    |  |                     |           |   |
| Sulfamethoxazole           | 21, 22  |   |                     |           |   |
| C7H5O4N3S                  | 3       |   |                     |           |   |
| S S A A A A A y            |         |   |                     |           |   |

<sup>1</sup>(Quaresma et al. 2019), <sup>2</sup>(Tay et al. 2011), <sup>3</sup>(Xu et al. 2019), <sup>4</sup>(Acero et al. 2000), <sup>5</sup>(Beltrán et al. 1998), <sup>6</sup>(Barletta et al. 2003), <sup>7</sup>(Sui et al. 2017), <sup>8</sup>(Azais et al. 2017), <sup>9</sup>(McDowell et al. 2005), <sup>10</sup>(Hübner et al. 2014), <sup>11</sup>(Hörsing et al. 2012), <sup>12</sup>(Merel et al. 2017), <sup>13</sup>(Rosal et al. 2009), <sup>14</sup>(Feng et al. 2008), <sup>15</sup>(Borowska et al. 2016), <sup>16</sup>(Keen et al. 2014), <sup>17</sup>(Miao et al. 2015), <sup>18</sup>(Favier et al. 2015), <sup>19</sup>(Diehle et al. 2019), <sup>20</sup>(Hermes et al. 2020), <sup>21</sup>(Willach et al. 2017), <sup>22</sup>(Martín de Vidales et al. 2012), <sup>23</sup>(Abellan et al. 2008), <sup>24</sup>(Rodayan et al. 2010), <sup>25</sup>(Gomez-Ramos et al. 2011), <sup>26</sup>(Gao et al. 2014), <sup>27</sup>(Hu et al. 2017), <sup>28</sup>(Bollmann et al. 2016), <sup>29</sup>(Zimmermann et al. 2012), <sup>30</sup>(Zucker et al. 2018), <sup>31</sup>(Lester et al. 2013), <sup>32</sup>(Lajeunesse et al. 2013).

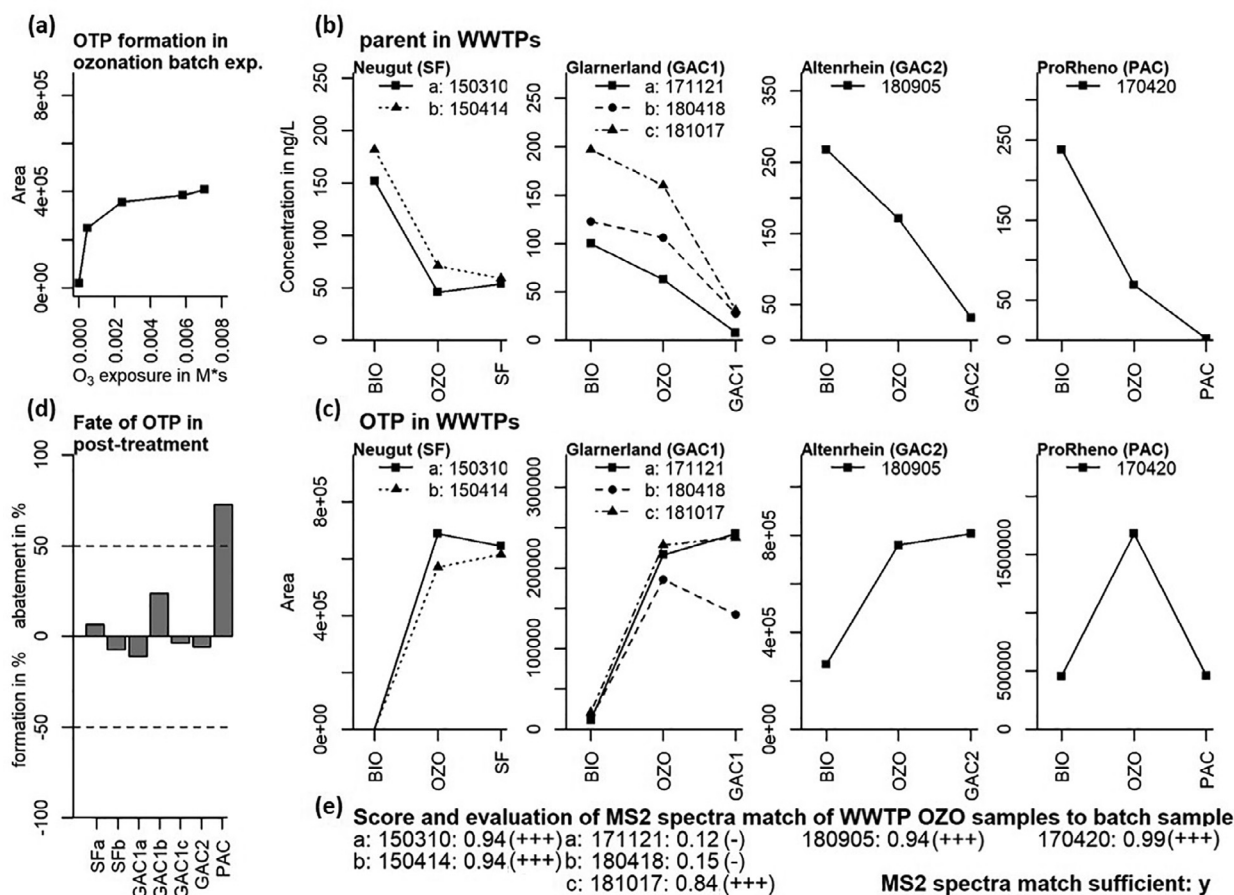


**Fig. 3.** Fate of irbesartan and the OTP IRB\_p\_195.1491\_12.8 (for structure see Fig. 2b) during biological treatment (BIO), ozonation (OZO) and post-treatment (SF/GAC1/GAC2/PAC) (a) Formation of the OTP in the ozonation batch experiment O3bAll, (b) fate of the parent irbesartan and (c) the OTP in the samples from four different WWTPs, (d) evaluation of the abatement of the OTP in the different post-treatments, and (e) MS<sup>2</sup> spectra evaluation of the OTP: the score of MS<sup>2</sup> spectra match between each WWTP OZO sample and the reference spectra of a batch sample, and an overall evaluation of the sufficiency of the match (see Section 2.5.2 for details). Sample numbers show sampling date (yyymmdd). Post-treatment were a sand filter (SF), GAC1 sampled at a: 16,000, b: 25,000, and c: 35,000 bed volumes, GAC2 sampled at 48,000 bed volumes, and PAC dosed with 13 mg/L onto a SF.

fenpropidin, lidocaine, sulpride, tramadol, and venlafaxine were also detected in the current study (Table 1). For clindamycin, the formation of a sulfoxide (S-oxide) from the thioether was observed. Hydroxylation can occur via reaction with  $\cdot\text{OH}$  at aromatic rings forming a phenol, on an aliphatic carbon or on a nitrogen and was observed in 13 OTPs. Since phenols react further quickly during ozonation (von Sonntag and von Gunten 2012) and therefore are unlikely to be found, hydroxylations are expected to mostly occur on aliphatic carbons through various  $\cdot\text{OH}$ -induced pathways (von Sonntag and Schuchmann 1997) (in 10 OTPs) (Table 1). A modification of  $(-\text{H}_2+\text{O})$  can be assigned to a formation of a carbonyl group (11 OTPs) or an aldehyde (7 OTPs); for another 10 OTPs this modification could not be definitively assigned. Such modifications were observed for aliskiren, bezafibrate, carbamazepine (Azais et al. 2017, Hübner et al. 2014, McDowell et al. 2005), citalopram, caffeine (Rosal et al. 2009), cyprodinil, diclofenac, fenpropidin, flufenamic acid, gabapentin, lidocaine, phenazone (Favier et al. 2015, Miao et al. 2015), propylamide, rosvastatin, sitagliptin (Hermes et al. 2020), tramadol, venlafaxine, and the sartans (Diehle et al. 2019) (Table 1). The same modification was observed in sitagliptin for the potential formation of a nitroso- or an oxime-group from the primary amine (also postulated by Hermes et al. (2020)). A modification of  $(-\text{H}_2+\text{O}_2)$  can be observed for the formation of a carboxylic acid, as detected in 13 OTPs of aliskiren, candesartan, carbamazepine (Azais et al. 2017, Hübner et al. 2014, McDowell et al. 2005), fenfluramine, flecainide,

irbesartan, lidocaine, phenazone (Miao et al. 2015), propylamide, sitagliptin (Hermes et al. 2020), and valsartan (Diehle et al. 2019) (Table 1). Benzisothiazolone was transformed into an OTP with a benzoquinone-type structure with the same atomic modification, which could occur via an ozone reaction of a phenol, which is formed as a transient product by ozone and/or  $\cdot\text{OH}$  (Ramseier and von Gunten 2009, Tentscher et al. 2018). Ten more OTPs showed the addition of oxygen atoms that could not be precisely localized, especially in OTPs after a cleavage of the molecule (for candesartan, carbamazepine, clindamycin, diclofenac, flufenamic acid, levamisole, mefenamic acid, and rosvastatin) (Table 1). The modification  $(-\text{H}_2+\text{O}_2)$  can also be a combination of a formation of a carbonyl group and the addition of a hydroxyl group. It also occurs in the transformation of a primary amine to a nitro group, which is a common reaction pathway (Lim et al. 2019), and was observed for 2 OTPs of sitagliptin (Hermes et al. 2020), 3 OTPs of sulfamethoxazole (Abellan et al. 2008, Gao et al. 2014, Gomez-Ramos et al. 2011, Rodayan et al. 2010, Willach et al. 2017), and 1 OTP of amisulpride (here from an aniline-type moiety, which is not very common). A modification of  $(-\text{H}_2)$  occurs by a transformation of an alcohol to a carbonyl group via H-abstraction at the C-H by  $\cdot\text{OH}$ , formation of a peroxy radical from the reaction of the carbon-centered radical with oxygen and the formation of the corresponding carbonyl compound (von Sonntag and Schuchmann 1997), as in OTPs of oxazepam and potentially of aliskiren and sucralose (Hu et al. 2017). An abstraction of hydrogen atoms was observed in 6 more OTPs,

which cannot be easily explained. An transformation of a C-C or C-N bond to a double bond is not likely. An exception is the formation of chlorothiazide from hydrochlorothiazide by the oxidation of a C-N bond (Borowska et al. 2016). The modification of (-H<sub>2</sub>) observed in 5 OTPs (for aliskiren, N-desmethyltramadol, lidocaine, and sitagliptin (Hermes et al. 2020)) is unclear. Finally, the formation of a sulfonic acid (-H<sub>2</sub>+O<sub>3</sub>) was found for levamisole (Table 1).

### 3.3.3. Abatement of parent MP and formation of OTPs

In Fig 3a, the evolution of irbesartan OTP IRB\_p\_195.1491\_12.8 is shown in the O3bAll experiment. It is formed quickly and peak area remains rather stable with increasing ozone exposure. For other OTPs (Text S6, SI), a continuous formation or a formation followed by a decrease can be observed.

The concentrations of the corresponding parent compound irbesartan after biological treatment (BIO), ozonation (OZO), and post-treatment in the four investigated WWTPs are shown in Fig 3b. Irbesartan, as well as most other investigated MPs, were still present after biological treatment in all measurement campaigns of the four WWTPs. The selected MPs were abated to different extents during ozonation. In general, abatement was smaller in WWTPs Glarnerland and Altenrhein, since the specific ozone doses were lower (0.23-0.33 gO<sub>3</sub>/gDOC) compared to WWTP Neugut (0.5-0.55 gO<sub>3</sub>/gDOC). WWTP ProRhenno claimed to have applied low specific ozone doses (0.21 gO<sub>3</sub>/gDOC); however, the evaluation of parent MPs (here and in Krahnstöver et al. (2018)) revealed that the specific ozone doses must have been higher than planned. Please note that the quantification of the parent MPs included correction through internal standard in this study (27 of the 40 MPs had matching isotopically-labeled ISTD). However, no corrections for matrix factors or relative recoveries for MPs without matching ISTD were performed, to keep a rather similar level of uncertainty as for the OTP area estimation. Nevertheless, the results are in agreement with full quantification results (including recoveries) done elsewhere for selected MPs (Krahnstöver et al. 2018, Oltramare et al. 2021, Schollée et al. 2021b).

### 3.3.4. Fate of the OTP of irbesartan in different post-treatments

The fate of OTP IRB\_p\_195.1491\_12.8 of irbesartan in the post-treatments of the four WWTPs is shown in Fig. 3c. Different post-treatments were investigated: WWTP Neugut had a sand filter (SF), while the other WWTPs either had GAC filtration, sampled at different bed volumes (GAC1 at WWTP Glarnerland and GAC2 at WWTP Altenrhein), or PAC dosed onto a sand filter (at WWTP ProRhenno). IRB\_p\_195.1491\_12.8 was already present in small amounts in the BIO samples of some WWTPs. This can occur if the OTP is also formed during biological transformation in the human body or the activated sludge treatment. All transformation products that were not predominately increasing during the ozonation step were already filtered out during the processing of the data, because this study focuses only on OTPs. IRB\_p\_195.1491\_12.8 was mainly formed during ozonation in each WWTP. Different patterns were observed in the subsequent post-treatments. In WWTP Neugut, the peak area of the OTP was rather stable during sand filtration. In WWTP Glarnerland with GAC1 filtration, the OTP was abated to a certain extent or was stable, while in WWTP Altenrhein with GAC2 filtration at higher bed volumes, the OTP was stable. In WWTP ProRhenno with a PAC treatment, it was significantly abated. Since the fate of the OTPs in the different post-treatments is of special interest, the relative difference between the OZO and EFF (i.e., SF, GAC1, GAC2, and PAC) samples was further evaluated and illustrated in Fig. 3d for IRB\_p\_195.1491\_12.8. The relative difference was categorized as *abatement* if >50%, *stable* between 50% and -50%, and *formation* <-50%. A rather broad range of 50% to -50% was chosen as *stable* to account for the uncertainties of the estimated OTP peak areas, which arise through the

automatic fitting of the signal peaks, the lack of correction with internal standards and for matrix effects, and the lack of LOQ values. The fate of each OTP categorized as *abatement* (A), *stable* (S), and *formation* (F) in the seven different sampling campaigns is also summarized in Table 1 and will be further discussed below.

### 3.3.5. Verification of OTP occurrence in WWTPs via MS<sup>2</sup> spectra comparison

To confirm that an OTP signal in the WWTP samples and the ozonation batch samples truly originated from the same OTP precursor, the MS<sup>2</sup> spectra were compared. An MS<sup>2</sup> score was calculated for the OTP signal measured in the OZO sample of each WWTP campaign and a selected reference MS<sup>2</sup> spectrum of an ozonated batch sample. The results of the MS<sup>2</sup> spectra match for IRB\_p\_195.1491\_12.8 for all OZO samples are provided in Fig. 3e and was rated overall as sufficient (five out of the seven samples resulted in a very good MS<sup>2</sup> score; see Section 2.5.2. for details on categorization). The rating of the MS<sup>2</sup> spectra match for all OTPs is summarized in Table 1. From the 84 OTPs, the MS<sup>2</sup> spectra match was sufficient for 56. However, the remaining 28 OTPs might still be present in the WWTPs but possibly in low concentrations, leading to meaningless MS<sup>2</sup> spectra or with an interfering compound at a similar mass.

### 3.4. Overall fate of OTPs in the different post-treatments after ozonation

To assess the fate of OTPs during post-treatment, the 56 OTPs with sufficient MS<sup>2</sup> spectra matches were used. Fig. 4 illustrates the fate of these OTPs in the seven WWTP campaigns assigned according to their relative signal reduction into abatement (>50%), stable (between 50% and -50%), and formation (<-50%). Between 42 and 53 OTPs were identified in seven WWTP campaigns. These numbers can differ due to varying occurrence and concentration patterns of parent compounds in the wastewater effluents, and due to different specific ozone doses, pH of wastewater and matrix compositions.

At WWTP Neugut, which has a sand filtration as post-treatment, the result of the two campaigns were very consistent. Most (89%) of the 53 identified OTPs were stable during sand filtration. N-oxides, for example, and most other OTPs were found to have low abatement, as has been observed previously for ATE\_p\_283.1666\_21.2, LAM\_p\_259.9988\_13.7, PHE\_p\_165.1021\_17.6, and SMX\_n\_282.0188\_18.0 (Bollmann et al. 2016, Bourgin et al. 2018, Merel et al. 2017). Only 6% were abated, most probably through biotransformation, namely CBZ\_p\_251.0812\_17.9 (known as BQM, for which a biological transformation to BaQM and further to BaQD (here CBZ\_p\_283.0711\_17.3) was previously reported (Hübner et al. 2014)), FAD\_n\_232.0224\_21.7, FAD\_n\_258.038\_19.6, and LID\_p\_247.1438\_17.8. Furthermore, 6% of the identified OTPs were formed during post-treatment, which is possible if these transformation products are forming through biotransformation from either remaining parent MPs or other OTPs (e.g., OTP CBZ\_p\_283.0711\_17.3, above). A systematic evaluation of the abatement of OTPs in comparison to their parent MPs based on ozone-reactive functional groups was conducted in another study for ozonated surface water followed by a biological sand filter (Gulde et al. 2021).

At WWTP Glarnerland, a GAC filter (GAC1) was used as a post-treatment. Samples were taken at three different run times at (a) 16,000, (b) 25,000, and (c) 35,000 BV. With 40-58% abatement of the 42-43 identified OTPs, a better abatement was observed than in the biological sand filter (described above). Less OTPs (33-45%) were stable and 7-14% were formed. When comparing the abatement of OTPs as a function of the bed volumes treated, similar results were obtained at 16,000 and at 25,000 BV (23/25 OTPs



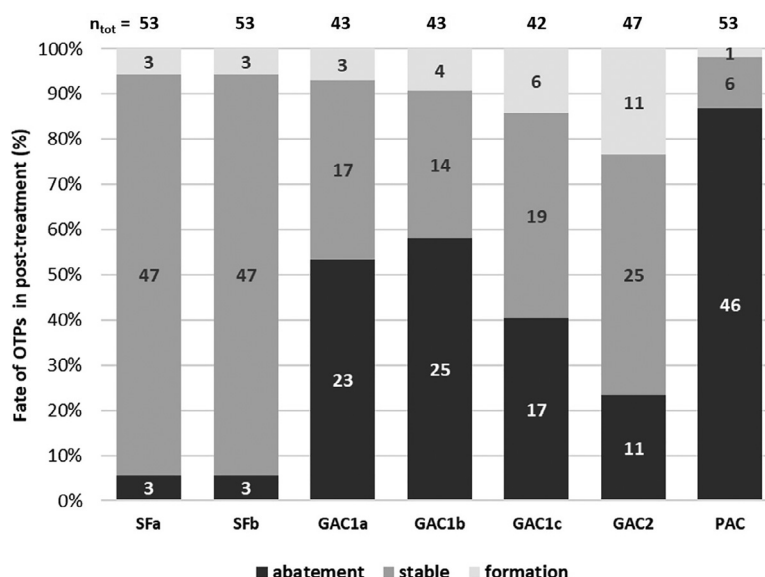


**Fig. 4.** Relative fate of OTPs in different post-treatment processes, assigned according to their relative signal reduction to three categories: abatement (>50%), stable (between 50% and -50%), and formation (<-50%). Two campaigns at WWTP Neugut with a biological sand filter (SFa and SFb), three campaigns at WWTP Glarnerland with a GAC filter sampled at GAC1a: 16,000 bed volumes (BV), GAC1b: 25,000 BV, GAC1c: 35,000 BV, one campaign at WWTP Altenrhein with a GAC filter (GAC2) sampled at 48,000 BV, and one campaign at WWTP ProRhenio with 13 mg/L PAC dosed onto a sand filter (PAC). The numbers of OTPs in the different categories are also indicated in the graph.

abated, 53/58%), but less abatement was observed at 35,000 BV (17 OTPs abated, 40%).

WWTP Altenrhein was also equipped with GAC filtration (GAC2) and was sampled once, at 48,000 BV. In this WWTP, the share of abatement was smaller (23%, 11 OTPs) than for WWTP Glarnerland. More OTPs were stable (53%, 25 OTPs) or formed (23%, 11 OTPs). This confirms the trend of less efficient OTP abatement with longer GAC filter run times, which can be explained by the lower sorption capacities of GAC filters over time (Crittenden et al. 2005). The OTPs chlorothiazide (HCT\_n\_293.9415\_10.8), tramadol *N*-oxide (TRA\_p\_280.1905\_14.4), and venlafaxine *N*-oxide (VEN\_p\_294.2064\_16.1) were found to sorb well on GAC, in agreement with Bourgin et al. (2018) and Knopp et al. (2016), and consequently showed also a clear drop of abatement at higher bed volumes. In addition to adsorption sites, GAC filters exhibit a biofilm that may enable biotransformation, which can enhance abatement (Reungoat et al. 2012). However, it is difficult to delineate sorption and biotransformation. Several OTPs that were formed in ozonation were also formed during GAC filtration. Four of them had a pronounced increase, with a tendency of higher formation with higher bed volumes: CAN\_p\_207.0766\_17.0, CBZ\_p\_283.0711\_17.3 (see also discussion of sand filtration above), DIC\_n\_257.9729\_16.7, and PHE\_p\_237.0868\_15.1. Most probably, these OTPs are also biotransformation products of the parent MPs or other OTPs.

In general, it can be concluded that GAC filtration is more efficient in abating OTPs than biological sand filtration. This is in agreement with a previous study based on a trend analysis of unknown OTP signals (Schollée et al. 2018). Note that in the WWTP with sand filtration, a higher specific ozone dose was used than in the WWTPs with GAC filtration, yielding different OTP peak areas, which may have partly biased the results.

In the WWTP ProRhenio, the ozonated water was treated with 13 mg/L PAC dosed onto a sand filter. The PAC performed significantly better than GAC or SF, with 87% abatement of OTPs (46 of 53 OTPs were abated). This result was expected because fresh PAC is continuously dosed to the sand filter, enabling better sorption of MPs and OTPs compared to a GAC filter, which loses adsorption capacity with increasing operation time.

#### 4. Conclusion

- Laboratory experiments with aqueous solutions containing acetate and methanol to simulate real water ozonation conditions ( $O_3$  /  $\bullet OH$  exposure,  $R_{ct}$ ) are adequate to mimic ozonation conditions in wastewater treatment and enable the detection of environmentally-relevant OTPs.
- Laboratory ozonation experiments with 87 micropollutants (MPs) were performed by dividing them into 19 “smart” MP mixtures. This approach allows identification of OTPs, as well as assignment of OTPs to their corresponding parent MPs, while reducing the number of necessary experiments and sample analyses.
- Two data-evaluation approaches for the identification of OTPs in WWTPs with aid of laboratory ozonation experiments were developed:
  - o Approach 1: LC-HR-MS signals formed in laboratory batch experiments were identified as OTP candidates for each parent MP. This resulted in a comprehensive list of OTP signals (1749 OTP signals for 70 MPs, without MS<sup>2</sup> spectra), which can be used for suspect screening in other studies. This approach was not further applied, but a workflow was proposed for the identification of OTPs in WWTPs.
  - o Approach 2: Relevant OTPs were identified by directly screening for LC-HR-MS signals that were present in the WWTP samples and were formed in the batch experiments. Even though a re-measurement of the samples was necessary for the acquisition of MS<sup>2</sup> spectra for OTP confirmation, this is a very efficient high-throughput approach.
- Eighty-four OTPs from 40 different MPs could be identified during ozonation of secondary wastewater effluents from four different WWTPs (specific ozone doses, 0.23–0.55 gO<sub>3</sub>/gDOC):
  - o Structure elucidation, via interpretation of MS<sup>2</sup> spectra and expert knowledge on ozone chemistry, revealed 6 confirmed structures (level 1, reference standard), 6 probable structures (level 2a, library spectrum match), 71 tentative candidate structures (level 3), and one exact mass of interest (level 5) (Schymanski et al. 2014). To the best of our knowledge, 48

(58%) of the OTPs with proposed structures have not been reported in literature previously.

- For 56 OTPs, their occurrence in the WWTP could be verified through MS<sup>2</sup> spectra comparison by calculating MS<sup>2</sup> scores. MS<sup>2</sup> spectra of most of the 84 OTPs were made publicly available in MassBank (2006) to extend the community knowledge and support the identification of OTPs.
- The overall abatement of the OTPs in the different post-treatments was poor in biological sand filtration, better in GAC columns (but with decreasing efficiency with higher bed volumes), and best in PAC treatment.
- Information on OTPs formed in laboratory systems with simulated water matrix or real systems should be used in future studies to better understand mechanisms of OTP formation during ozonation to include both ozone and hydroxyl radical reactions (Gulde et al. 2021). This will improve predictions and opens up the possibility to couple them to structural alerts for toxicity assessment (Lee et al. 2017, von Gunten 2018).

### Declaration of Competing Interest

The authors declare that they have no known competing financial interests or personal relationships that could have appeared to influence the work reported in this paper.

### Acknowledgements

Funding of Eawag discretionary fund, the waterworks Zurich (Stadt Zürich, Wasserversorgung WVV) and the Swiss Federal Office for the Environment FOEN (SCREEN-O3TP Project 00.0102.PZ / P403-1651) are acknowledged. We thank Elisabeth Salhi for her introduction into ozonation experiments and partners of several projects that provided samples and information: Max Schachtler (WWTP Neugut), Roberto Frei, Sandra Henneberger (WWTP ProRheno) and project team "Aktifilt Plus", Therese Krahnstöver and Thomas Wintgens (FHNW), Christoph Egli (WWTP Altenrhein) and Michael Thomann (Holinger AG), Klaus Biermann (WWTP Glarnerland), Marc Böhler, Marc Bourgin, Julian Fleiner, Antonio Hernandez, Christelle Oltramare, and Rebekka Teichler from Eawag.

### Supplementary materials

Supplementary material associated with this article can be found, in the online version, at doi:[10.1016/j.watres.2021.117200](https://doi.org/10.1016/j.watres.2021.117200).

### References

Abellan, M.N., Gebhardt, W., Schroder, H.F., 2008. Detection and identification of degradation products of sulfamethoxazole by means of LC/MS and -MSn after ozone treatment. *Water Sci. Technol.* 58 (9), 1803–1812.

Acero, J.L., Stemmler, K., von Gunten, U., 2000. Degradation Kinetics of Atrazine and Its Degradation Products with Ozone and OH Radicals: A Predictive Tool for Drinking Water Treatment. *Environ. Sci. Technol.* 34 (4), 591–597.

Azais, A., Mendret, J., Cazals, G., Petit, E., Brosillon, S., 2017. Ozonation as a pretreatment process for nanofiltration brines: Monitoring of transformation products and toxicity evaluation. *J. Hazard. Mater.* 338, 381–393.

Bader, H., Hoigné, J., 1981. Determination of ozone in water by the indigo method. *Water Res.* 15 (4), 449–456.

Barletta, B., Bolzacchini, E., Meinardi, S., Orlandi, M., Rindone, B., 2003. The kinetics and the mechanism of the reaction of 2-chloro-4,6-dialkylamino-1,3,5-triazines with ozone. *Ozone Sci. Eng.* 25, 81–94.

Beltrán, F.J., García-Araya, J.F., Álvarez, P.M., Rivas, J., 1998. Aqueous degradation of atrazine and some of its main by-products with ozone-hydrogen peroxide. *J. Chem. Technol. Biotechnol.* 71, 345–355.

Bollmann, A.F., Seitz, W., Prasse, C., Lucke, T., Schulz, W., Ternes, T., 2016. Occurrence and fate of amisulpride, sulpiride, and lamotrigine in municipal wastewater treatment plants with biological treatment and ozonation. *J. Hazard. Mater.* 320, 204–215.

Borowska, E., Bourgin, M., Hollender, J., Kienle, C., McArdell, C.S., von Gunten, U., 2016. Oxidation of cetirizine, fexofenadine and hydrochlorothiazide during ozonation: Kinetics and formation of transformation products. *Water Res.* 94, 350–362.

Bourgin, M., Beck, B., Boehler, M., Borowska, E., Fleiner, J., Salhi, E., Teichler, R., von Gunten, U., Siegrist, H., McArdell, C.S., 2018. Evaluation of a full-scale wastewater treatment plant upgraded with ozonation and biological post-treatments: Abatement of micropollutants, formation of transformation products and oxidation by-products. *Water Res.* 129, 486–498.

Brunner, A.M., Bertelkamp, C., Dingemans, M.M.L., Kolkman, A., Wols, B., Harmen, D., Siegers, W., Martijn, B.J., Oorthuizen, W.A., ter Laak, T.L., 2020. Integration of target analyses, non-target screening and effect-based monitoring to assess OMP related water quality changes in drinking water treatment. *Sci. Total Environ.* 705.

Carbajo, J.B., Petre, A.L., Rosal, R., Herrera, S., Leton, P., Garcia-Calvo, E., Fernandez-Alba, A.R., Perdigon-Melon, J.A., 2015. Continuous ozonation treatment of ofloxacin: Transformation products, water matrix effect and aquatic toxicity. *J. Hazard. Mater.* 292, 34–43.

Christophoridis, C., Nika, M.C., Aalizadeh, R., Thomaidis, N.S., 2016. Ozonation of ranitidine: Effect of experimental parameters and identification of transformation products. *Sci. Total Environ.* 557, 170–182.

Coelho, A.D., Sans, C., Agüera, A., Gomez, M.J., Esplugas, S., Dezotti, M., 2009. Effects of ozone pre-treatment on diclofenac: intermediates, biodegradability and toxicity assessment. *Sci. Total Environ.* 407 (11), 3572–3578.

Crittenden, J.C., Trussell, R.R., Hand, D.W., Howe, K.J., Tchobanoglous, G., 2005. *Water Treatment: Principles and Design*. John Wiley & Sons, Inc, Hoboken.

Diehle, M., Gebhardt, W., Pinnekamp, J., Schäffer, A., Linnemann, V., 2019. Ozonation of valsartan: Structural elucidation and environmental properties of transformation products. *Chemosphere* 216, 437–448.

El-taliawy, H., Casas, M.E., Bester, K., 2018. Removal of ozonation products of pharmaceuticals in laboratory Moving Bed Biofilm Reactors (MBBRs). *J. Hazard. Mater.* 347, 288–298.

Elovitz, M.S., von Gunten, U., 1999. Hydroxyl radical/ozone ratios during ozonation processes. I. The R(CT) concept. *Ozone Sci. Eng.* 21, 239–260.

Elovitz, M.S., von Gunten, U., Kaiser, H.P., 2000. Hydroxyl radical/ozone ratios during ozonation processes. II. The effect of temperature, pH, alkalinity, and DOM properties. *Ozone Sci. Eng.* 22, 123–150.

Faber, H., Lutze, H., Lareo, P.L., Frensemeier, L., Vogel, M., Schmidt, T.C., Karst, U., 2014. Liquid chromatography/mass spectrometry to study oxidative degradation of environmentally relevant pharmaceuticals by electrochemistry and ozonation. *J. Chromatogr. A* 1343, 152–159.

Favier, M., Dewil, R., Van Eyck, K., Van Schepdael, A., Cabooter, D., 2015. High-resolution MS and MS(n) investigation of ozone oxidation products from phenazone-type pharmaceuticals and metabolites. *Chemosphere* 136, 32–41.

Feng, J., Zheng, Z., Luan, J., Zhang, J., Wang, L., 2008. Degradation of diuron in aqueous solution by ozonation. *J. Environ. Sci. Health B* 43 (7), 576–587.

Gago-Ferrero, P., Schymanski, E.L., Bletsou, A.A., Aalizadeh, R., Hollender, J., Thomaidis, N.S., 2015. Extended Suspect and Non-Target Strategies to Characterize Emerging Polar Organic Contaminants in Raw Wastewater with LC-HRMS/MS. *Environ. Sci. Technol.* 49 (20), 12333–12341.

Gao, S., Zhao, Z., Xu, Y., Tian, J., Qi, H., Lin, W., Cui, F., 2014. Oxidation of sulfamethoxazole (SMX) by chlorine, ozone and permanganate—a comparative study. *J. Hazard. Mater.* 274, 258–269.

Gomez-Ramos, M.D.M., Mezcuá, M., Agüera, A., Fernandez-Alba, A.R., Gonzalo, S., Rodriguez, A., Rosal, R., 2011. Chemical and toxicological evolution of the antibiotic sulfamethoxazole under ozone treatment in water solution. *J. Hazard. Mater.* 192 (1), 18–25.

Gulde, R., Clerc, B., Rutsch, M., Helbing, J., Salhi, E., McArdell, C.S. and von Gunten, U. (2021) Micropollutant transformation during ozonation of surface water: Formation of transformation products and their fate during biological post-filtration. in preparation.

Gulde, R., Helbling, D.E., Scheidegger, A., Fenner, K., 2014. pH-Dependent Biotransformation of Ionizable Organic Micropollutants in Activated Sludge. *Environ. Sci. Technol.* 48 (23), 13760–13768.

Gulde, R., Meier, U., Schymanski, E.L., Kohler, H.P.E., Helbling, D.E., Derrer, S., Rentsch, D., Fenner, K., 2016. Systematic Exploration of Biotransformation Reactions of Amine-Containing Micropollutants in Activated Sludge. *Environ. Sci. Technol.* 50 (6), 2908–2920.

Hermes, N., Jewell, K.S., Falás, P., Lutze, H.V., Wick, A., Ternes, T.A., 2020. Ozonation of Sitagliptin: Removal Kinetics and Elucidation of Oxidative Transformation Products. *Environ. Sci. Technol.* 54, 10588–10598.

Hollender, J., Rothardt, J., Radny, D., Loos, M., Epting, J., Huguenberger, P., Borer, P., Singer, H., 2018. Comprehensive micropollutant screening using LC-HRMS/MS at three riverbank filtration sites to assess natural attenuation and potential implications for human health. *Water Res.* X 1.

Hörsing, M., Kosjek, T., Andersen, H.R., Heath, E., Ledin, A., 2012. Fate of citalopram during water treatment with O<sub>3</sub>, ClO<sub>2</sub>, UV and Fenton oxidation. *Chemosphere* 89 (2), 129–135.

Hu, R., Zhang, L., Hu, J., 2017. Investigation of ozonation kinetics and transformation products of sucralose. *Sci. Total Environ.* 603–604, 8–17.

Hübner, U., Seiwert, B., Reemtsma, T., Jekel, M., 2014. Ozonation products of carbamazepine and their removal from secondary effluents by soil aquifer treatment - Indications from column experiments. *Water Res.* 49, 34–43.

Hübner, U., von Gunten, U., Jekel, M., 2015. Evaluation of the persistence of transformation products from ozonation of trace organic compounds - A critical review. *Water Res.* 68, 150–170.

Itzel, F., Baetz, N., Hohrenk, L.L., Gehrman, L., Antakyal, D., Schmidt, T.C., Tuerk, J., 2020. Evaluation of a biological post-treatment after full-scale ozonation at a municipal wastewater treatment plant. *Water Res.* 170.

- Kamath, D., Mezyk, S.P., Minakata, D., 2018. Elucidating the Elementary Reaction Pathways and Kinetics of Hydroxyl Radical-Induced Acetone Degradation in Aqueous Phase Advanced Oxidation Processes. *Environ. Sci. Technol.* 52 (14), 7763–7774.
- Keen, O.S., Ferrer, I., Michael Thurman, E., Linden, K.G., 2014. Degradation pathways of lamotrigine under advanced treatment by direct UV photolysis, hydroxyl radicals, and ozone. *Chemosphere* 117, 316–323.
- Knopp, G., Prasse, C., Ternes, T.A., Cornel, P., 2016. Elimination of micropollutants and transformation products from a wastewater treatment plant effluent through pilot scale ozonation followed by various activated carbon and biological filters. *Water Res* 100, 580–592.
- Krahnstöver, T., Wintgens, T., Deininger, P., 2018. Spurenstoffentfernung durch die Kombination von Ozonung und Pulveraktivkohleabsorption mit anschließender Raumfiltration («Aktifit Plus»). Fachhochschule Nordwestschweiz FHNW, Muttenz.
- Krauss, M., Singer, H., Hollender, J., 2010. LC-high resolution MS in environmental analysis: from target screening to the identification of unknowns. *Anal. Bioanal. Chem.* 397 (3), 943–951.
- Lajeunesse, A., Blais, M., Barbeau, B., Sauvé, S., Gagnon, C., 2013. Ozone oxidation of antidepressants in wastewater—Treatment evaluation and characterization of new by-products by LC-QToFMS. *Chem. Cent. J.* 7 (15).
- Lee, M., Blum, L.C., Schmid, E., Fenner, K., von Gunten, U., 2017. A computer-based prediction platform for the reaction of ozone with organic compounds in aqueous solution: kinetics and mechanisms. *Environ. Sci. Process. Impacts* 19, 465–476.
- Lee, Y., Gerrity, D., Lee, M., Bogeat, A.E., Salhi, E., Gamage, S., Trenholm, R.A., Wert, E.C., Snyder, S.A., von Gunten, U., 2013. Prediction of Micropollutant Elimination during Ozonation of Municipal Wastewater Effluents: Use of Kinetic and Water Specific Information. *Environ. Sci. Technol.* 47 (11), 5872–5881.
- Lee, Y., Kovalova, L., McArdell, C.S., von Gunten, U., 2014. Prediction of micropollutant elimination during ozonation of a hospital wastewater effluent. *Water Res* 64, 134–148.
- Lee, Y., von Gunten, U., 2016. Advances in predicting organic contaminant abatement during ozonation of municipal wastewater effluent: reaction kinetics, transformation products, and changes of biological effects. *Environ. Sci. Water Res. Technol.* 2 (3), 421–442.
- Lester, Y., Mamane, H., Zucker, I., Avisar, D., 2013. Treating wastewater from a pharmaceutical formulation facility by biological process and ozone. *Water Res* 47 (13), 4349–4356.
- Lim, S., McArdell, C.S., von Gunten, U., 2019. Reactions of aliphatic amines with ozone: Kinetics and mechanisms. *Water Res* 157, 514–528.
- Magdeburg, A., Stalter, D., Schlüsener, M., Ternes, T., Oehlmann, J., 2014. Evaluating the efficiency of advanced wastewater treatment: Target analysis of organic contaminants and (geno-) toxicity assessment tell a different story. *Water Res* 50, 35–47.
- Margot, J., Kienle, C., Magnet, A., Weil, M., Rossi, L., de Alencastro, L.F., Abegglen, C., Thonney, D., Chèvre, N., Schärer, M., Barry, D.A., 2013. Treatment of micropollutants in municipal wastewater: Ozone or powdered activated carbon? *Sci. Total Environ.* 461–462, 480–498.
- Martín de Vidales, M.J., Robles-Molina, J., Domínguez-Romero, J.C., Cañizares, P., Sáez, C., Molina-Díaz, A., Rodrigo, M.A., 2012. Removal of sulfamethoxazole from waters and wastewaters by conductive-diamond electrochemical oxidation. *J. Chem. Technol. Biotechnol.* 87 (10), 1441–1449.
- MassBank (2006) High Quality Mass Spectral Database, <https://massbank.eu/>.
- Mathon, B., Coquery, M., Liu, Z., Penru, Y., Guillon, A., Esperanza, M., Miège, C., Choubert, J.-M., 2021. Ozonation of 47 organic micropollutants in secondary treated municipal effluents: Direct and indirect kinetic reaction rates and modelling. *Chemosphere* 262, 127969.
- McArdell, C.S., Böhler, M., Hernandez, A., Oltramare, C., Büeler, A. and Siegrist, H. (2020) Pilotversuche zur erweiterten Abwasserbehandlung mit granulierter Aktivkohle (GAK) und kombiniert mit Teilozonung (O3/GAK) auf der ARA Glarnerland (AVG), Ergänzende Untersuchungen zur PAK-Dosierung in die biologische Stufe mit S::Select®-Verfahren in Kombination mit nachfolgender GAK, Final report, Eawag, Dübendorf, <https://www.dora.lib4ri.ch/eawag/islandora/object/eawag%3A21543>.
- McDowell, D.C., Huber, M.M., Wagner, M., von Gunten, U., Ternes, T.A., 2005. Ozonation of Carbamazepine in Drinking Water: Identification and Kinetic Study of Major Oxidation Products. *Environ. Sci. Technol.* 39 (20), 8014–8022.
- Merel, S., Lege, S., Yanez Heras, J.E., Zwiener, C., 2017. Assessment of N-Oxide Formation during Wastewater Ozonation. *Environ. Sci. Technol.* 51 (1), 410–417.
- Mestankova, H., Escher, B., Schirmer, K., von Gunten, U., Canonica, S., 2011. Evolution of algal toxicity during (photo)oxidative degradation of diuron. *Aquat. Toxicol.* 101 (2), 466–473.
- Mestankova, H., Schirmer, K., Canonica, S., von Gunten, U., 2014. Development of mutagenicity during degradation of N-nitrosamines by advanced oxidation processes. *Water Res* 66, 399–410.
- Mestankova, H., Schirmer, K., Escher, B.I., von Gunten, U., Canonica, S., 2012. Removal of the antiviral agent oseltamivir and its biological activity by oxidative processes. *Environ. Pollut.* 161, 30–35.
- Miao, H.F., Cao, M., Xu, D.Y., Ren, H.Y., Zhao, M.X., Huang, Z.X., Ruan, W.Q., 2015. Degradation of phenazone in aqueous solution with ozone: influencing factors and degradation pathways. *Chemosphere* 119, 326–333.
- Oltramare, C., Hernandez, A., Mangold, S., Boehler, M. and McArdell, C.S. (2021) Abatement of micropollutants in granular activated carbon (GAC) filters with and without pre-ozonation in a pilot scale study, in preparation.
- Phungsai, P., Kurisu, F., Kasuga, I., Furumai, H., 2016. Molecular characterization of low molecular weight dissolved organic matter in water reclamation processes using Orbitrap mass spectrometry. *Water Res* 100, 526–536.
- Quaresma, A.V., Sousa, B.A., Silva, K.T.S., Silva, S.Q., Werle, A.A., Afonso, R., 2019. Oxidative treatments for atenolol removal in water: Elucidation by mass spectrometry and toxicity evaluation of degradation products. *Rapid Commun. Mass Spectrom.* 33 (3), 303–313.
- Ramseier, M.K., von Gunten, U., 2009. Mechanisms of Phenol Ozonation-Kinetics of Formation of Primary and Secondary Reaction Products. *Ozone Sci. Eng.* 31 (3), 201–215.
- Reungoat, J., Escher, B.I., Macova, M., Argand, F.X., Gernjak, W., Keller, J., 2012. Ozonation and biological activated carbon filtration of wastewater treatment plant effluents. *Water Res* 46 (3), 863–872.
- Rodayan, A., Roy, R., Yargeau, V., 2010. Oxidation products of sulfamethoxazole in ozonated secondary effluent. *J. Hazard. Mater.* 177 (1–3), 237–243.
- Rodayan, A., Segura, P.A., Yargeau, V., 2014. Ozonation of wastewater: Removal and transformation products of drugs of abuse. *Sci. Total Environ.* 487, 763–770.
- Rosal, R., Rodriguez, A., Perdigon-Melon, J.A., Petre, A., Garcia-Calvo, E., Gomez, M.J., Agüera, A., Fernandez-Alba, A.R., 2009. Degradation of caffeine and identification of the transformation products generated by ozonation. *Chemosphere* 74 (6), 825–831.
- Schindler Wildhaber, Y., Mestankova, H., Scharer, M., Schirmer, K., Salhi, E., von Gunten, U., 2015. Novel test procedure to evaluate the treatability of wastewater with ozone. *Water Res* 75, 324–335.
- Schollée, J.E. (2017) MSMSsim: functions for processing HRMS2 spectra from output from RMassBank, mainly for calculating spectral similarity, <https://github.com/dutchjes/MSMSsim>.
- Schollée, J.E., Bourgin, M., von Gunten, U., McArdell, C.S., Hollender, J., 2018. Non-target screening to trace ozonation transformation products in a wastewater treatment train including different post-treatments. *Water Res* 142, 267–278.
- Schollée, J.E., Gulde, R., von Gunten, U. and McArdell, C.S. (2021a) High-throughput screening of predicted ozonation transformation products in wastewater through *in silico* fragmentation, in preparation.
- Schollée, J.E., Hollender, J., McArdell, C.S., 2021. Characterization of advanced wastewater treatment with ozone and activated carbon using LC-HRMS based non-target screening with automated trend assignment. *Water Research* doi:10.1016/j.watres.2021.117209.
- Schollée, J.E., Schymanski, E.L., Stravs, M.A., Gulde, R., Thomaidis, N.S., Hollender, J., 2017. Similarity of High-Resolution Tandem Mass Spectrometry Spectra of Structurally Related Micropollutants and Transformation Products. *J. Am. Soc. Mass Spectrom.* 28 (12), 2692–2704.
- Schymanski, E.L., Jeon, J., Gulde, R., Fenner, K., Ruff, M., Singer, H.P., Hollender, J., 2014. Identifying Small Molecules via High Resolution Mass Spectrometry: Communicating Confidence. *Environ. Sci. Technol.* 48 (4), 2097–2098.
- Sein, M.M., Zedda, M., Tuerk, J., Schmidt, T.C., Gollock, A., von Sonntag, C., 2008. Oxidation of diclofenac with ozone in aqueous solution. *Environ. Sci. Technol.* 42 (17), 6656–6662.
- Staehelin, J., Hoigne, J., 1985. Decomposition of ozone in water in the presence of organic solutes acting as promoters and inhibitors of radical chain reactions. *Environ. Sci. Technol.* 19 (12), 1206–1213.
- Stalter, D., Magdeburg, A., Weil, M., Knacker, T., Oehlmann, J., 2010. Toxication or detoxication? In vivo toxicity assessment of ozonation as advanced wastewater treatment with the rainbow trout. *Water Res* 44 (2), 439–448.
- Stefan, M.I., Bolton, J.R., 1998. Mechanism of the degradation of 1,4-dioxane in dilute aqueous solution using the UV hydrogen peroxide process. *Environ. Sci. Technol.* 32 (11), 1588–1595.
- Stefan, M.I., Mack, J., Bolton, J.R., 2000. Degradation pathways during the treatment of methyl tert-butyl ether by the UV/H2O2 process. *Environ. Sci. Technol.* 34 (4), 650–658.
- Sui, Q., Gebhardt, W., Schroder, H.F., Zhao, W., Lu, S., Yu, G., 2017. Identification of New Oxidation Products of Bezafibrate for Better Understanding of Its Toxicity Evolution and Oxidation Mechanisms during Ozonation. *Environ. Sci. Technol.* 51 (4), 2262–2270.
- Tay, K.S., Rahman, N.A., Abas, M.R.B., 2011. Characterization of atenolol transformation products in ozonation by using rapid resolution high-performance liquid chromatography/quadrupole-time-of-flight mass spectrometry. *Microchem. J.* 99 (2), 312–326.
- Tentscher, P.R., Bourgin, M., von Gunten, U., 2018. Ozonation of Para-Substituted Phenolic Compounds Yields p-Benzoquinones, Other Cyclic alpha,beta-Unsaturated Ketones, and Substituted Catechols. *Environ. Sci. Technol.* 52 (8), 4763–4773.
- von Gunten, U., 2003. Ozonation of drinking water: Part I. Oxidation kinetics and product formation. *Water Res* 37 (7), 1443–1467.
- von Gunten, U., 2018. Oxidation Processes in Water Treatment: Are We on Track? *Environ. Sci. Technol.* 52, 5062–5075.
- von Gunten, U., Hoigné, J., 1994. Bromate Formation during Ozonation of Bromide-Containing Waters: Interaction of Ozone and Hydroxyl Radical Reactions. *Environ. Sci. Technol.* 28 (7), 1234–1242.
- von Sonntag, C., Schuchmann, H.-P., 1997. In: Alfassi, Z.B. (Ed.), *The Chemistry of Free Radicals: Peroxyl Radicals*. Wiley & Sons Ltd, pp. 173–234.
- von Sonntag, C., von Gunten, U., 2012. *Chemistry of ozone in water and wastewater treatment: From basic principles to applications*. IWA Publishing, London.
- Willach, S., Lutze, H.V., Eckey, K., Loppenberg, K., Luling, M., Terhalle, J., Wolbert, J.B., Jochmann, M.A., Karst, U., Schmidt, T.C., 2017. Degradation of sulfamethoxazole using ozone and chlorine dioxide - Compound-specific stable isotope analy-

- sis, transformation product analysis and mechanistic aspects. *Water Res* 122, 280–289.
- Xu, Z., Xie, M., Ben, Y., Shen, J., Qi, F., Chen, Z., 2019. Efficiency and mechanism of atenolol decomposition in Co-FeOOH catalytic ozonation. *J. Hazard. Mater.* 365, 146–154.
- Zimmermann, S.G., Schmukat, A., Schulz, M., Benner, J., von Gunten, U., Ternes, T.A., 2012. Kinetic and Mechanistic Investigations of the Oxidation of Tramadol by Ferrate and Ozone. *Environ. Sci. Technol.* 46 (2), 876–884.
- Zimmermann, S.G., Wittenwiler, M., Hollender, J., Krauss, M., Ort, C., Siegrist, H., von Gunten, U., 2011. Kinetic assessment and modeling of an ozonation step for full-scale municipal wastewater treatment: Micropollutant oxidation, by-product formation and disinfection. *Water Res* 45 (2), 605–617.
- Zucker, I., Mamane, H., Riani, A., Gozlan, I., Avisar, D., 2018. Formation and degradation of N-oxide venlafaxine during ozonation and biological post-treatment. *Sci. Total Environ.* 619–620, 578–586.